Ore Geology Reviews 103 (2018) 21–37

Contents lists available at ScienceDirect

Ore Geology Reviews

journal homepage: www.elsevier.com/locate/oregeo

Compositional evolution of the tetrahedrite solid solution in porphyry-epithermal system: A case study of the Baimka Cu-Mo-Au trend, Chukchi Peninsula, Russia

L.I. Marushchenko [a,*], I.A. Baksheev [a,*], E.V. Nagornaya [a], A.F. Chitalin [b], Yu.N. Nikolaev [a], E.A. Vlasov [a]

[a] Geology Department, Lomonosov Moscow State University, Leninskiye Gory GSP-1, 119234 Moscow, Russia
[b] Institute of Geotechnology, LLC, MSU Science Park, 1, Leninskiye Gory street, bld. 77, 119234 Moscow, Russia

ARTICLE INFO

Article history:
Received 14 December 2015
Accepted 17 January 2017
Available online 19 January 2017

Keywords:
Porphyry-epithermal system
Tetrahedrite solid solution
Baimka trend
Chukchi Peninsula
Russia

ABSTRACT

The Peschanka deposit and Nakhodka ore field occurring in the Baimka Cu-Mo-Au porphyry-epithermal trend in the western Chukchi Peninsula, Russia are spatially related to monzonitic rocks of the Early Cretaceous Egdykgych Complex. Tetrahedrite solid solution (Tt_s) was recognized at the deposit and within the ore field in the following assemblages: (1) porphyry stage bornite, chalcopyrite, and molybdenite, (2) transitional (subepithermal) stage sphalerite, galena, chalcopyrite, and As-free pyrite, (3) HS epithermal stage enargite, chalcopyrite and high-fineness native gold, and (4) IS epithermal stage As-rich pyrite, galena, sphalerite, and low-fineness native gold and electrum. The porphyry and subepithermal Tt_s crystals are oscillatory zoned because of variable contents of Sb and As. The literature data show that similar zoning has been recognized in the Tt_s crystals in the other porphyry Cu-Mo-Au and transitional assemblages and differs from the other type deposits. Therefore, such a zoning is considered to be a guide to these two mineralization types. No zoning was found in Tt_s referred to the HS and IS epithermal assemblages within the Baimka trend. The porphyry stage Tt_s evolves from Fe-rich tennantite ((sb = Sb/(Sb + As) below 0.01, fe = Fe/(Fe + Zn) 0.60–0.80) through oscillatory zoned tennantite enriched in Sb and Zn (sb 0.19–0.37, fe 0.56–0.66) to tetrahedrite enriched in Zn (sb 0.51–0.70, fe 0.39–0.66). This trend is caused by the Sb accumulation and increased f_{S2}. The review of published data shows that such trend is typical of the other porphyry deposit worldwide. Therefore, it is considered to be a guide to distinguish porphyry deposits from the other type deposits containing fahlores and to distinguish porphyry-stage fahlores. The composition of the transitional stage Tt_s evolves from Zn-rich tetrahedrite (sb 0.56–0.82, fe 0.03–0.05) through Zn-rich tennantite (sb 0.03–0.19, fe 0.11–0.13) followed by Zn-rich oscillatory zoned solid solution (sb 0.03 to 0.69, fe 0.09 to 0.11) to goldfieldite. This evolution testifies to increased f_{Te2} to the end of transitional stage. The HS stage Tt_s corresponds to Fe-rich tennantite (sb below 0.05, fe 0.65–1.00) containing high Cu_{excess} (1.43 apfu). The IS stage Tt_s evolves from Zn-rich tennantite (sb = 0, fe = 0.44) to Zn-rich tetrahedrite (sb = 0.97, fe = 0.03). The latest Zn-rich tetrahedrite of this assemblage is enriched in Ag (up to 4.1 wt.%) testifying to increasing Ag activity to the end of mineralizing process. The review of literature data shows the similar trend for the transitional and IS Tt_s in the other porphyry-epithermal systems. Therefore the Tt_s evolution trend is a criterion to separate porphyry, transitional, IS, and HS Tt_s.

1. Introduction

The tetrahedrite group minerals $^{[III]}A_6^{[IV]}B_6(^{[III]}X^{[IV]}Y_3)_4^{[VI]}Z$, where A = Cu, Ag, B = Cu, Ag, Fe, Zn, X = Sb, As, Bi, Te, and Y and Z = S, Se (Moëlo et al., 2008) are typical of sulfide mineralization present in many hydrothermal ore deposits (Mozgova and Tsepin, 1983a, b). Owing to wide isomorphic substitutions and various types of hydrothermal deposits where tetrahedrite solid solution (Tt_s) has been found, the composition of the tetrahedrite-group minerals is susceptible to the mineralizing conditions. These minerals are found at epi- and mesothermal gold deposits, base metal deposits, VHMS deposits, and in porphyry-epithermal systems (Mozgova and Tsepin, 1983a,b; Sack et al., 2003; Spiridonov et al., 2005, 2009). In the porphyry-epithermal system, the tetrahedrite group minerals are formed at all stages of mineralization: porphyry,

* Corresponding authors.
E-mail address: Luba.rogacheva@gmail.com (L.I. Marushchenko).

http://dx.doi.org/10.1016/j.oregeorev.2017.01.018
0169-1368/

transitional (subepithermal), and HS (high sulfidation), IS (intermediate sulfidation), and LS (low sulfidation) epithermal. Tt_s associated with the porphyry stage minerals was established at the El Teniente, Chile (Araya et al., 1997) and Kedabek, Azerbaijan (Bortnikov et al., 1993) porphyry deposits. Tt_s associated with the base-metal sulfides was found at the deposits and prospects of the Birgilida-Tomino ore cluster, Russia (Plotinskya et al., 2014, 2015), Bugdaya porphyry Mo-W deposit, Russia (Kovalenker et al., 2011), various deposits in Bulgaria and Greece (Voudouris et al., 2013; Repstock et al., 2016). Epithermal tetrahedrite-group minerals were reported by Kovalenker et al. (1986), Fadda et al. (2005), Alfieris (2006), and Catchpole et al. (2012). Researchers having reported chemical composition of the tetrahedrite-group minerals from porphyry-epithermal systems do not focus frequently on mineralization stages (porphyry, transitional, epithermal).

This article discusses the tetrahedrite-group minerals of the porphyry, transitional and epithermal stages from the Peschanka deposit and Nakhodka ore field occurring in the Baimka Cu-Mo-Au porphyry-epithermal trend in the western Chukchi Peninsula, Russia. These findings have been used to attempt to establish criteria to distinguish mineralization stages associated with variations in the composition of the tetrahedrite solid solution and to show differences of tetrahedrite solid solution related to the porphyry-epithermal system from other deposits.

1.1. Geological setting

Peschanka the largest porphyry-gold-copper deposit in Russia and Nakhodka ore field are the members of the Baimka porphyry Cu-Mo-Au trend located about 200 km south of Bilibino, western Chukchi Peninsula (Fig. 1a). The indicated resources of the Peschanka deposit estimated by IMC Montan according to the JORC Code for copper equivalent (CuEq) cut-off grade of 0.4% are as follows: 1208 Mt of ore, 6.39 Mt of copper, 165.4 kt of molybdenum, 345.7 t of gold, 3.44 kt of silver (average grades are 0.53% Cu, 0.014 % Mo, 0.29 g/t Au, 2.6 g/t Ag) (Chitalin et al., 2013).

The Nakhodka ore field comprises the Vesenny gold deposit and Malysh, Nakhodka, Vesenny III, and Pryamoy deposits. The inferred mineral resources of the Nakhodka and Pryamoy deposits estimated by IMC Montan according to the JORC Code for CuEq cut-off grade of 0.3% are as follows: 917.9 Mt of ore, 3.1 Mt of copper, 50 kt of molybdenum, 278 t of gold, and 1.13 kt of silver (average grades are: 0.34% Cu, 0.0054% Mo, 0.30 g/t Au, and 1.2 g/t Ag). The inferred mineral resources of the Vesenny deposit as veins are as follows 4.38 Mt of ore, 14.9 t of gold, and 137.6 t of silver (average grades are 3.4 g/t Au and 31.4 g/t Ag). Those resources as stockwork for gold equivalent cut-off grade of 1 g/t are as follows: 65.74 Mt of ore, 97.1 t of gold, 895.5 t of silver (average grades are 1.48 g/t Au and 13.6 g/t Ag). Thus total gold and silver resources are 112 and 1033 t, respectively (Chitalin et al., 2013).

The Baimka trend elongated for more than 90 km (Fig. 1b) is part of the Oloi metallogenic zone, where Cu-Mo-Au porphyry-epithermal systems were formed in magmatic arc environment. This trend comprises Upper Jurassic and Lower Cretaceous stratified volcanic and terrigenous sequences intruded by igneous rocks of various composition and age. The Late Jurassic gabbro is the most ancient. Then, large bodies of porphyry diorite and monzonitoids of the Early Cretaceous Egdykgych Complex with the U/Pb zircon age of 139–143 Ma (Kotova et al., 2012; Baksheev et al., 2014; Moll-Stalcup et al., 1995) age were emplaced (Figs. 2 and 3). The Cu-Mo-Au-porphyry systems are related to the quartz monzonite porphyry stocks of the Egdykgich Complex. The Upper Jurassic sequences are folded and intruded by the Late Jurassic and Early Cretaceous intrusions and all these rocks are unconformably overlain in places by the sediments of the Early Cretaceous Ainakhkurgen Formation. The post-ore Late Cretaceous basaltic subvolcanic bodies and andesitic dikes are the youngest rocks in the trend (except for Quaternary alluvium).

Structural features of the Baimka trend indicate that it is a regional-scale dextral strike-slip fault zone formed under latitudinal horizontal extension and meridional compression. Echelon-like meridional extension zones within the Baimka Fault Zone control localization of the Early Cretaceous plutons, porphyry dikes and stocks, metasomatic rocks, and mineralized stockworks of the magmatic porphyry ore system. Latest NW-SE trending dextral strike-slip faults and conjugate SW-NE-trending sinistrial strike-slip faults transect the porphyry deposits.

Four types of wall-rock alteration were identified at the deposits within the Baimka trend from early to late: (1) quartz-biotite-potassium feldspar (potassic), (2) propylitic, (3) quartz-sericite divided into two subtypes: quartz-chlorite-muscovite (QSR I) and quartz-phengite-muscovite-dolomite ± (QSR-II), and (4) argillic (Marushchenko et al., 2015; Nagornaya, 2013).

Potassic alteration predominant at the Peschanka deposit forms an internal metasomatic aureole with negligible Cu-Mo mineralization. Propylitic alteration found at all deposits forms an outer metasomatic aureole replacing both intrusive and country rocks. Quartz-sericite alteration of the both subtypes forms zones cutting

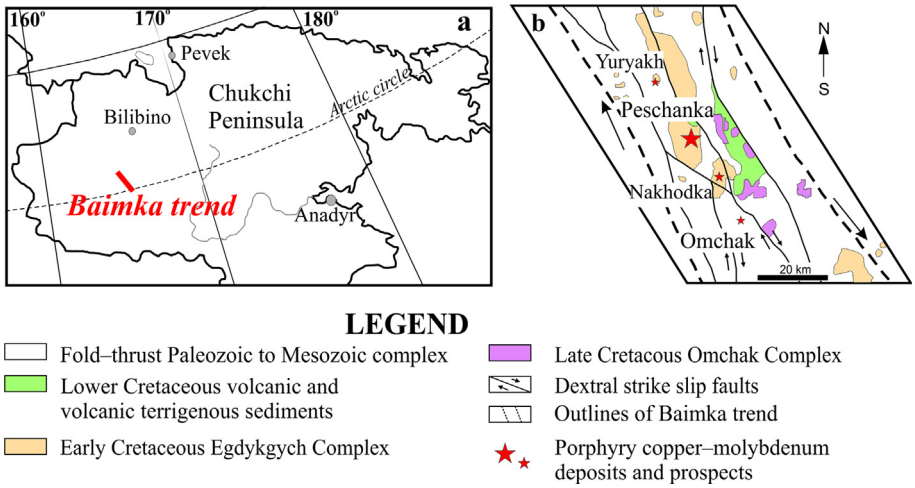

Fig. 1. Geographical location (a) and general geological scheme (b) of Baimka Cu-Mo-Au trend.

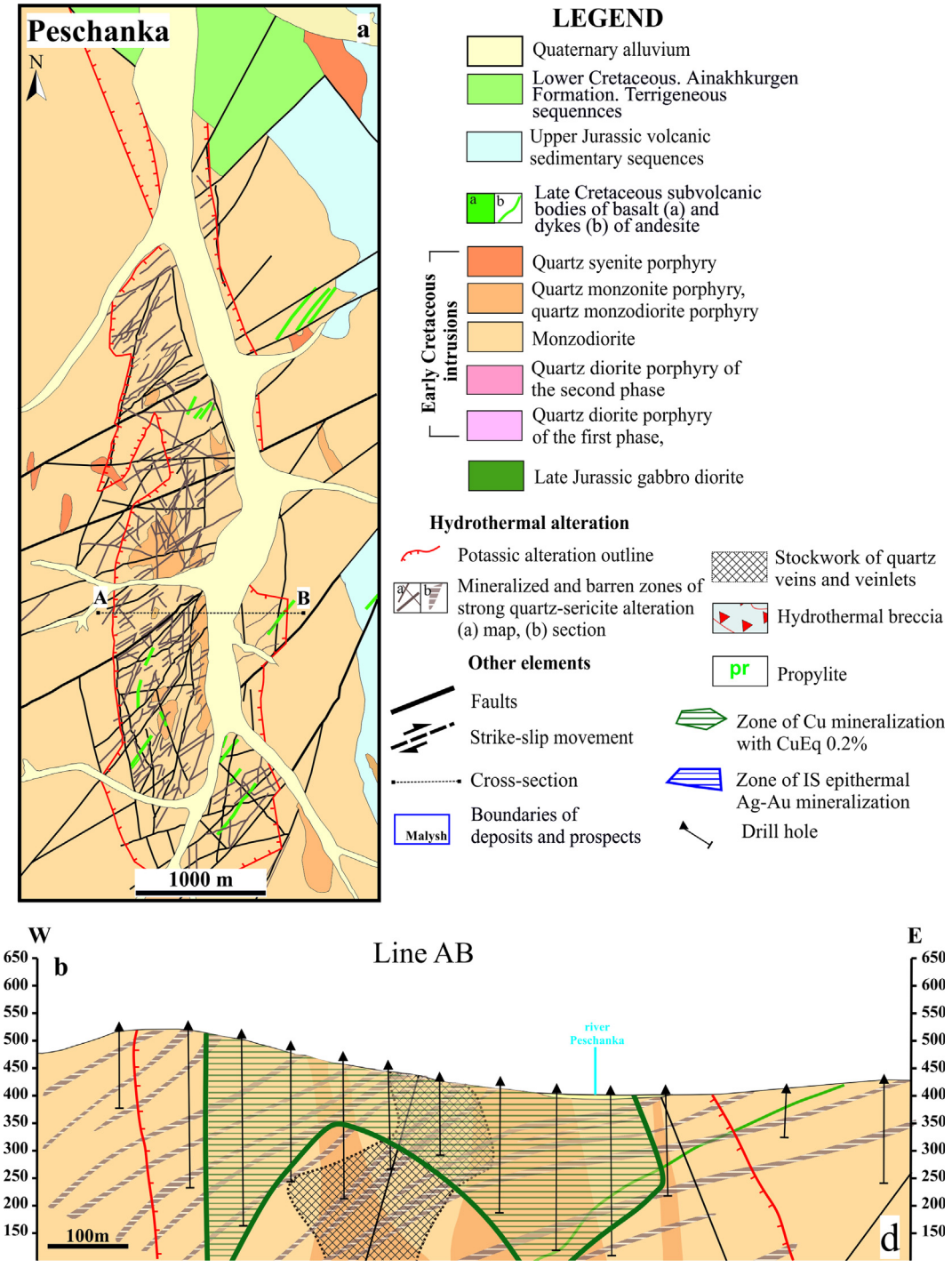

Fig. 2. Simplified geological map (a) and cross-section (b) of Peschanka deposit.

potassic alteration at the Peschanka deposit, while in the Nakhodka ore field it is the most abundant. Argillic alteration composed of illite, quartz and Mn-rich carbonates is the most abundant within the Nakhodka ore field where it accompanies epithermal precious metal mineralization at the Vesenny deposit. Argillic alteration at the Peschanka deposit is barren.

Porphyry Cu-Mo mineralization is spatially related to QSR I alteration is impregnation and stockwork quartz veins and veinlets with bornite, chalcopyrite, molybdenite, and unzoned As-free pyrite (Fig. 4a). The tetrahedrite group minerals, and Se-bearing galena, clausthalite, and native gold occur as rare inclusions in bornite. The model Re/Os age of molybdenite from Peschanka and the Nakhodka field of 142.6 ± 6.9 and 143.3 ± 3.0 Ma, respectively (Baksheev et al., 2014) is close within uncertainty to the U/Pb zircon age of the Egdykgich Complex.

Transitional (subepithermal) mineralization spatially related to QSR II occurs as veins and veinlets cutting all earlier alteration (Fig. 4b). Unzoned As-free pyrite, galena and sphalerite are the major ore minerals; chalcopyrite and tetrahedrite group minerals are minor; negligible hessite, petzite and native gold with the fineness of 759 to 850 are enclosed within chalcopyrite. As typical of the HS epithermal mineralization, mineralization, enargite occurs

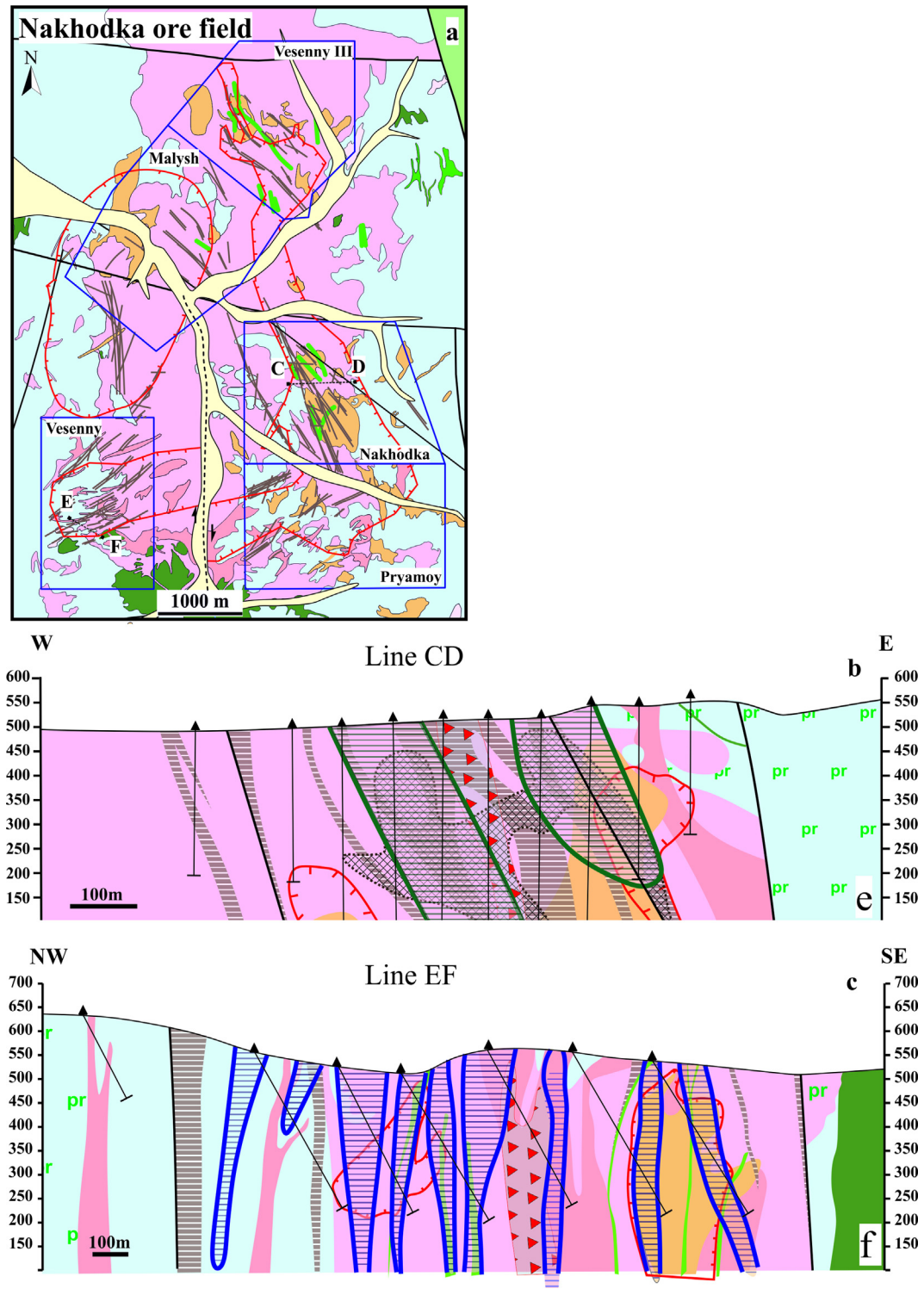

Fig. 3. Simplified geological map (a) and cross sections (b, c) of the Nakhodka ore field. See Fig. 2 for legend.

with tennantite and quartz veins and veinlets related to the both subtypes of quartz-sericite alteration host sporadic high-fineness native gold (910–953). However, no gangue minerals characteristic of the HS mineralization (alunite, dickite, APS minerals) were identified.

Economic IS epithermal gold mineralization in the classification of Sillitoe and Hedenquist (2003) or low sulfidation carbonate-base metal Au mineralization in that of Corbett and Leach (1998) within the Baimka trend identified at the southern flank of the Nakhodka ore field at the Vesenny deposit and Pryamoy deposit is spatially related to illite-quartz-Mn-rich dolomite-rhodochrosite argillic rock (Fig. 4c). Zoned As-rich pyrite (up to 10 wt% As), sphalerite, galena, and Zn-rich Tt_s are the major ore constituents; electrum (657–743), low-fineness native gold (756–857), and hessite are minor; stützite, pearceite, and Cu-bearing acanthite are rare. Native gold and electrum close intergrown with hessite are enclosed and fill fractures in pyrite, galena and Tt_s (Nagornaya et al., 2012).

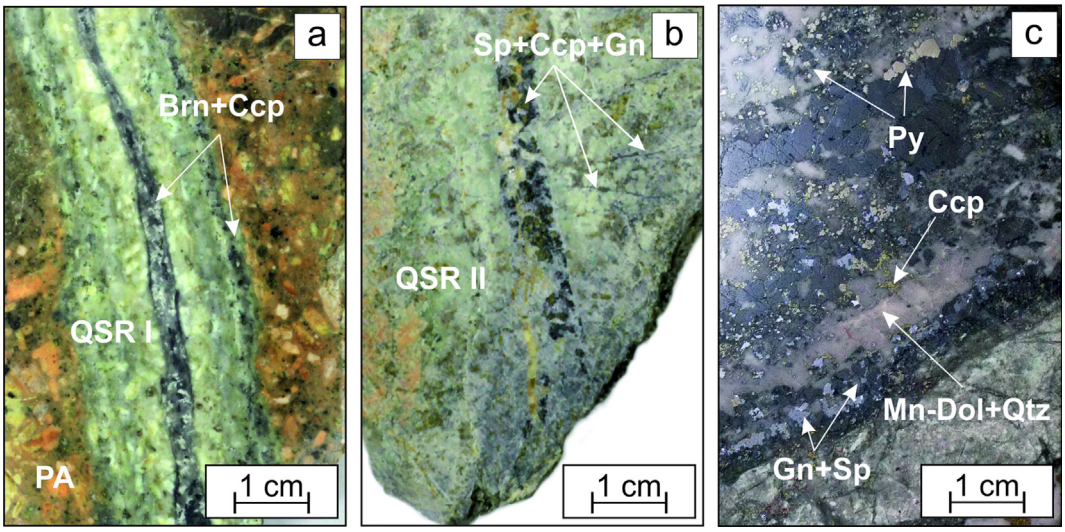

Fig. 4. Photos of the major type alterations and ores. (a) Quartz-muscovite alteration (QSR I) accompanied by the porphyry bornite-chalcopyrite mineralization replaces potassic alteration, Peschanka deposit; (b) quartz-phengite-muscovite alteration (QSR II) penetrated by the transitional stage As-free pyrite-sphalerite-galena-chalcopyrite veinlets, Peschanka deposit; (c) the IS stage quartz–Mn-rich dolomite-rhodochrosite vein with As-rich pyrite, galena, and sphalerite, Vesenny deposit. Abbreviations: Brn = bornite, Ccp = chalcopyrite, Gn = galena, QSR I = quartz-chlorite-muscovite rock, QSR II = quartz-phengite-muscovite altered rocks with tourmaline, PA = potassic alteration, Py = pyrite, Sp = sphalerite, Qtz = quartz.

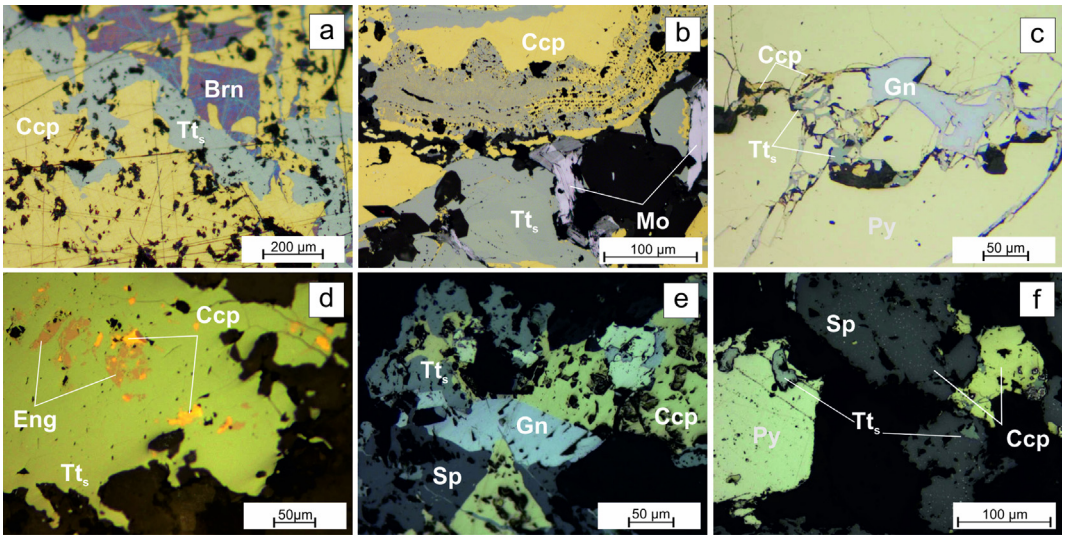

Fig. 5. Photomicrographs of sulfide minerals: (a, b) porphyry, (c) transitional, (d) HS epithermal, and (e, f) IS epithermal assemblages of (a, b, c) Peschanka deposit and(d, e, f) Nakhodka ore field: (d) Pryamoy prospect, (e, f) Vesenny deposit. (a) Tetrahedrite solid solution filling fractures in chalcopyrite overgrows and replaces bornite, (b) intergrowth of tetrahedrite solid solution and early chalcopyrite overgrown by late chalcopyrite; early chalcopyrite is associated with molybdenite, (c) brecciated crystals of As-free pyrite cemented by the aggregate of chalcopyrite, galena, and Tt_s, (d) relics of enargite and chalcopyrite within the grains of Tt_s, (e) Tt_s overgrowing chalcopyrite, sphalerite, and galena and cementing breciated pyrite grain, (f) Tt_s filling fractures in pyrite, chalcopyrite, and sphalerite. *Abbreviations:* Eng = enargite, Tt_s = tetrahedrite solid solution. See Fig. 2 for other abbreviations.

Table 1
Assemblages of ore minerals from deposits and occurrences within Baimka trend.

Stage	Mineral assemblages
EARLY PORPHYRY (Mo)	Chalcopyrite, molybdenite, pyrite
LATE PORPHYRY (CuAu)	Bornite, chalcopyrite, pyrite, clausthalite, Se-rich galena, Fe-rich tennantite up to Zn-rich tetrahedrite, high-fineness native gold, chalcocite group*, native copper*
TRANSITIONAL (SUBEPITHERMAL)	Pyrite, galena, sphalerite, chalcopyrite, Zn-rich tennantite - tetrahedrite, froodite, altaite, petzite, goldfieldite, hessite, petzite, low-fineness native gold, electrum
IS EPITHERMAL (CARBONATE – BASE-METAL AU)	As-bearing pyrite, sphalerite, chalcopyrite, galena, Zn-rich tennantite – tetrahedrite, electrum, low-finesses native gold, hessite, petzite, altaite, native tellurium, clausthalite, stützite, pearceite, acanthite
HS EPITHERMAL	Enargite, Cu-rich tennantite, high-fineness native gold
LS EPITHERMAL	Pb-Bi-Se-Te minerals, Ag-Te-Se minerals, kurilite, arsenopyrite, algodonite, Se-bearing pearceite, naumannite, marcasite, cinnabar
SUPERGENE	Chalcocite group minerals*, native copper*, covellite, azurite, copper sulfate

This table is based on Nagornaya (2013) Nikolaev et al. (2016) and our unpublished data.
* Denotes that origin of the chalcocite group minerals and native copper cannot be clearly identified on the basis of available data alone. Formation of these minerals is possible at both mentioned stages.

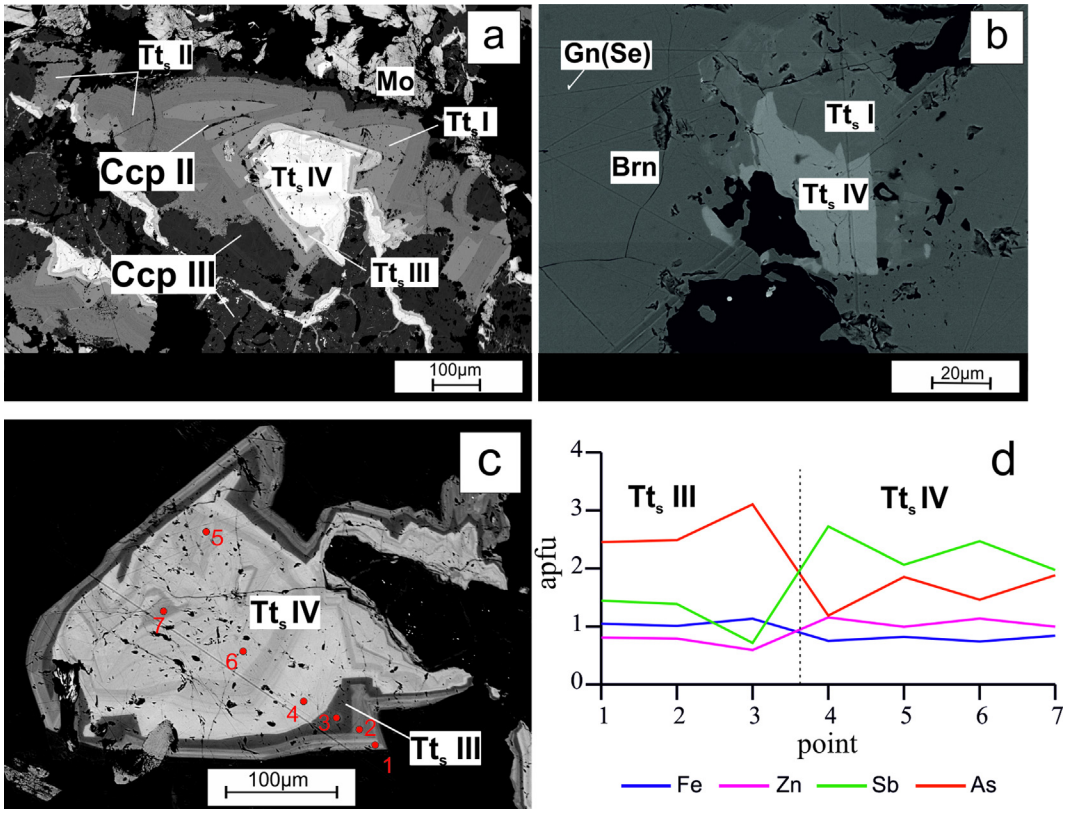

Fig. 6. (a–c) Back-scattered electron images of porphyry-stage Tts. from the Peschanka deposit. (a) Tt_s I and II intergrown with chalcopyrite II and replaced by zoned Tt_s III and IV and chalcopyrite III; chalcopyrite III is cut by stringers of tetrahedrite solid solution III and IV, (b) Tt_s I replaces bornite and in turn is replaced by Tt_sIV, (c) magnified fragment of Fig. a, (d) variations in the Sb, As, Fe, and Zn concentrations along profile within zoned crystal shown in Fig. a; numbers correspond to analyzed points in Table 2. Gn(Se) = galena rich in Se. See Figs. 2 and 3 for other abbreviations.

Table 2
Representative electron microprobe data for porphyry- and transitional stage tennantite-tetrahedrite solid solution series from Baimka trend.

Stage	Porphyry				Transitional (subepithermal)								
Deposit	Peschanka				Peschanka							Nakhodka	Malysh
Generation	I		III	IV		I	II	III	IV	V	Tn(Bi)		
Comp. wt%	1 bornite	2 ccp	3	4 bornite	5 ccp	6	7	8	9	10	11	12	13
Cu	47.09	28.48	41.51	40.51	39.80	38.79	39.01	43.25	41.94	44.19	39.56	40.97	38.65
Ag	0.14	0.11	0.10	0.13	0.38	bdl	bdl	0.05	bdl	0.42	bdl	0.74	0.29
Fe	2.65	4.57	3.81	2.28	4.47	0.25	0.30	0.83	2.94	0.08	1.07	0.88	bdl
Zn	2.03	1.96	3.43	4.92	3.37	7.49	7.60	7.88	7.31	0.62	7.23	7.20	7.16
As	18.72	19.24	11.96	6.23	8.45	3.80	4.87	18.05	18.99	9.11	14.80	15.80	2.86
Sb	bdl	0.06	11.45	21.04	15.97	24.63	23.53	2.31	0.10	bdl	bdl	6.45	26.39
Te	bdl	bdl	bdl	bdl	bdl	bdl	bdl	bdl	0.05	16.60	bdl	bdl	bdl
Bi	bdl	bdl	bdl	bdl	bdl	bdl	bdl	bdl	bdl	bdl	9.83	0.06	bdl
S	28.21	28.48	27.51	25.83	26.71	25.07	25.48	27.53	28.78	25.73	26.10	28.04	24.96
Total	98.84	99.08	99.77	100.94	98.98	100.03	100.79	99.91	100.11	96.75	98.47	100.14	100.31
Formula calculated on the basis of 29 atoms													
Cu(A)	9.981	10	9.985	9.981	9.879	10	9.953	9.993	9.682	9.936	9.971	9.757	9.056
Ag	0.019	0	0.015	0.019	0.056	0	0	0.007	0	0.064	0	0.104	0.044
Cu(B)	1.036	0.369	0.055	0.197	0	0.032	0	0.209	0	1.493	0	0	0.103
Fe	0.705	1.211	1.047	0.652	1.261	0.074	0.087	1.807	0.772	0.024	0.307	0.238	0
Zn	0.462	0.444	0.807	1.201	0.812	1.883	1.885	3.611	1.640	0.156	1.771	1.667	1.811
As	3.715	3.801	2.454	1.328	1.779	0.834	1.054	0.285	3.718	1.999	3.162	3.192	0.632
Sb	0	0.007	1.446	2.759	2.070	3.325	3.134	0	0.012	0	0	0.802	3.584
Te	0	0	0	0	0	0	0	0	0.006	2.137	0	0	0
Bi	0	0	0	0	0	0	0	0	0	0	0.754	0.004	0
S	13.082	13.152	13.192	12.863	13.143	12.853	12.887	12.867	13.169	13.191	13.035	13.236	12.870
fe	0.60	0.73	0.56	0.35	0.61	0.04	0.04	0.11	0.32	0.13	0.15	0.13	0
sb	0	0	0.37	0.68	0.54	0.80	0.75	0.07	0	0	0	0.2	0.85
Cu_{tot}	11.017	10.369	10.040	10.177	9.879	10.032	9.953	10.202	9.682	11.429	9.971	9.752	10.059

brn and **ccp** denote that Tt_s replaces bornite and chalcopyrite, respectively; second generation Tt_s is not shown because of fail in correct measurement of its composition, Tn (Bi) denotes tennantite enriched in Bi, **bdl** denotes that content of element is below detection limit. ***fe*** = Fe/(Fe + Zn); ***sb*** = Sb/(Sb + As)

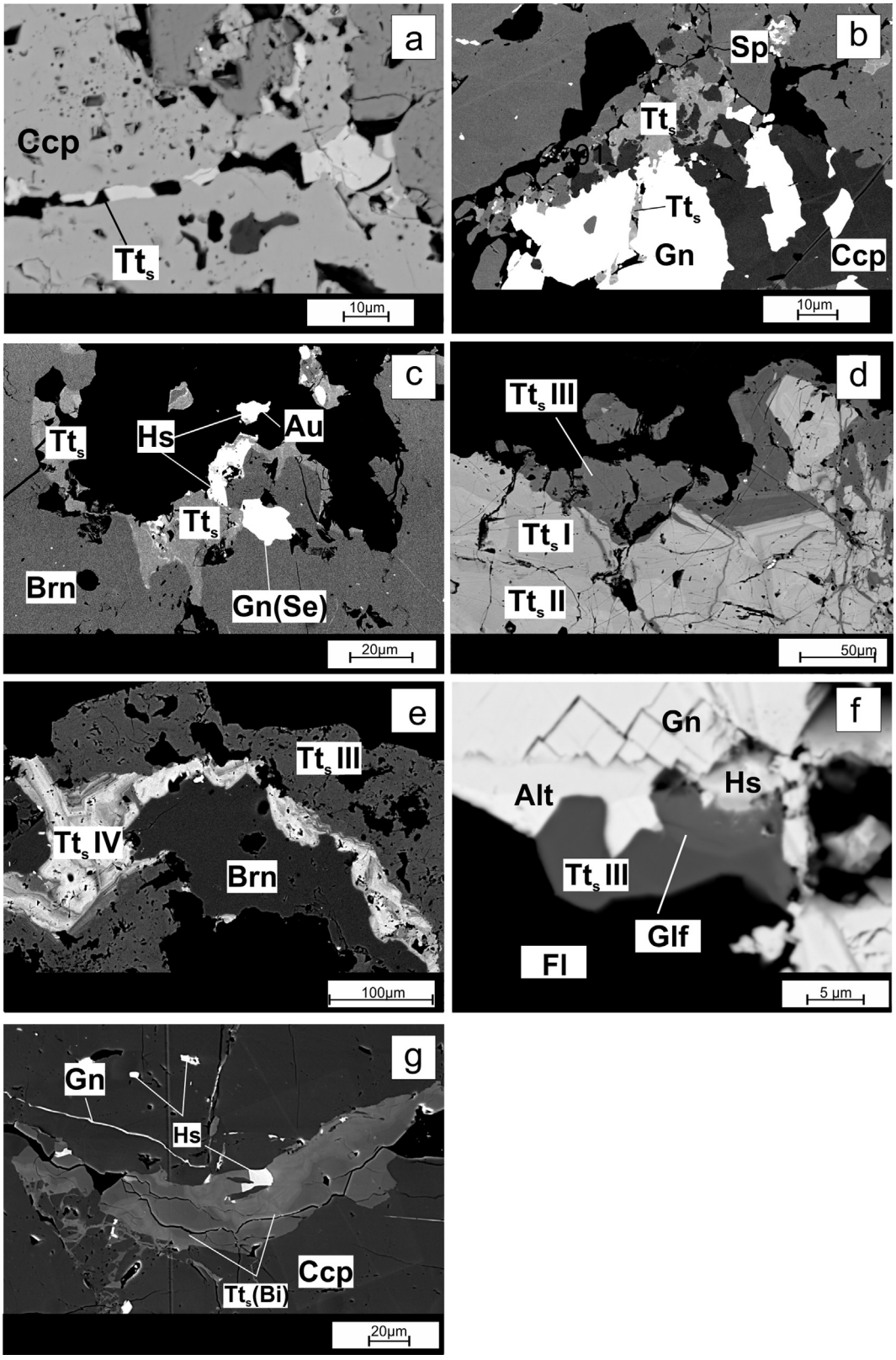

Fig. 7. Back-scattered electron images of the transitional-stage Tt_s from the Peschanka deposit. (a) Tt_s fills fracture in chalcopyrite, (b) Tt_s fills fractures in galena and overgrows sphalerite, (c) Tt_s associated with hessite and low-fineness gold replaces bornite; bornite contains exsolved Se-bearing galena, (d) aggregate of complexly zoned grains showing three generations of transitional Tt_s, (e) oscillatory zoned Tt_s IV replacing Tt_s III and bornite, (f) Tt_s III overgrowing galena is replaced by goldfieldite (Tt_s V) under effect of late Te- and Ag-solutions, which also caused the precipitation of hessite and altaite, (g) Bi-bearing tennantite associated with hessite fills fracture in chalcopyrite; chalcopyrite is cut by galena stringers. Alt = altaite, Au = native gold, Glf = goldfieldite, Fl = fluorite, Hs = hessite. Tt_s(Bi) = Tt_s rich in Bi. See Figs. 2 and 3 for other abbreviations.

1.2. Methods

An electron microscopic study and determination of chemical composition of Tt_s were performed on a Jeol JSM-6480LV scanning electron microscope equipped with an Inca-Energy 350 EDS and Inca-Wave 500 WDS operated at acceleration voltage of 20 kV and current intensity 2 nA at the Laboratory of Analytical Techniques of High Spatial Resolution, Department of Petrology, Moscow State University. The chemical composition of Tt_s has been measured on a Camebax SX-50 electron microprobe at the Department of Mineralogy of the same university and verified on a Jeol JXA-8230 electron microprobe at the same laboratory. A Camebax SX-50 electron microprobe was operated at acceleration voltage of 20 kV and current intensity of 30 nA. The following standards were used: hessite (Ag), sphalerite (Zn, S), FeAsS (Fe), nadorite (Sb), FeAsS (As), alabandine (Mn), molybdenite (Mo), PbS (Pb), CdSe (Se), coloradoite (Te), Bi_2S_3 (Bi), covellite (Cu). A Jeol JXA-8230 electron microprobe was operated at acceleration voltage of 20 kV and current intensity 20 nA. The following standards were used: Ag metallic (Ag), sphalerite (Zn, S), pyrite (Fe), Sb_2S_3 (Sb), As (As), ZnSe (Se), PbTe (Te), Bi_2S_3 (Bi), Cu metallic (Cu).

The Tt_s chemical formulae were calculated of the basis of 29 atoms. The Cu_{excess} value was calculated as $Cu_{tot} - {}^{A}Cu$, where ${}^{A}Cu$ is 10 – Ag. The *sb* and *fe* values were calculated from apfu as follows Sb/(Sb + As) and Fe/(Fe + Zn), respectively The tetrahedrite-group minerals were named according to classification of Moëlo et al. (2008).

2. Results

At the Peschanka deposit and in the Nakhodka ore field, the tetrahedrite-group minerals were found as typical, but minor constituents in the following assemblages: (1) porphyry stage bornite, chalcopyrite, and molybdenite (Fig. 5a,b), (2) transitional stage sphalerite, galena, As-free pyrite, and chalcopyrite (Fig. 5c), (3) rare HS epithermal stage enargite, chalcopyrite, and high-fineness gold (Fig. 5d), and (4) IS epithermal or carbonate–base-metal Au stage As-bearing pyrite, sphalerite, galena, and low-fineness gold to electrum (Fig. 5e,f). All mineral assemblages found within the Baimka trend are given in Table 1.

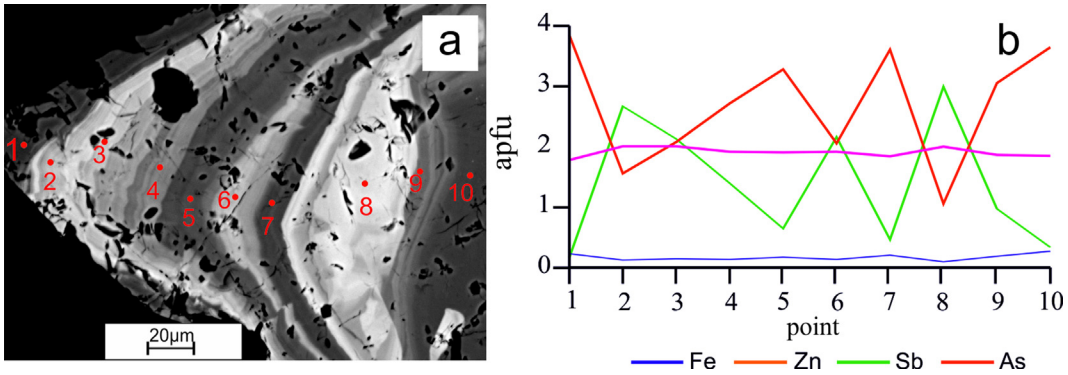

Fig. 8. Variations in the Sb, As, Fe, and Zn concentrations along profile within zoned crystal of the transitional stage Tt_s. Numbers correspond to analyzed points in Table 1A.

Table 3
Representative electron microprobe data for epithermal HS and IS stage tennantite-tetrahedrite solid solution series from Baimka trend.

Stage	Epithermal HS				Epithermal IS			
Deposit	Pryamoy	Peschanka			Vesenny		Pryamoy	
Comp., wt%								
Cu	48.82	49.07	43.51	47.31	39.88	36.22	42.64	39.80
Ag	0.05	bdl	bdl	0.23	0.60	4.19	0.08	0.98
Fe	7.88	3.68	4.83	4.78	2.97	2.15	1.32	0.79
Zn	bdl	0.11	0.10	bdl	7.81	6.80	7.65	7.36
As	16.30	19.93	13.09	20.10	21.29	9.11	19.48	12.64
Sb	0.15	bdl	10.60	0.14	1.18	15.78	0.86	11.71
Te	bdl	bdl	0.09	bdl	0.13	bdl	bdl	bdl
Bi	bdl	bdl	bdl	bdl	0.05	bdl	bdl	bdl
S	26.61	27.35	26.74	27.91	26.00	25.06	27.44	26.64
Total	100.61	100.15	98.96	100.42	99.91	98.26	99.47	99.92
Formula calculated on the basis of 29 atoms								
Cu (A)	9.993	10	10	9.969	9.520	9.265	9.989	9.777
Ag	0.007	0	0	0.031	0.084	0.631	0.011	0.142
Cu (B)	1.382	1.433	0.623	0.979	0	0	0.066	0
Fe	2.088	0.976	1.342	1.259	0.807	0.626	0.354	0.221
Zn	0	0.025	0.024	0	1.812	1.691	1.753	1.757
As	3.221	3.938	2.711	3.945	4.311	1.977	3.896	2.634
Sb	0.018	0	1.351	0.017	0.147	2.107	0.106	1.501
Te	0	0	0.011	0	0.015	0	0	0
Bi	0	0	0	0	0.004	0	0	0
S	12.291	12.628	12.939	12.800	12.300	12.704	12.824	12.969
fe	1.00	0.98	0.98	1.00	0.31	0.27	0.17	0.11
sb	0.01	0.00	0.33	0.00	0.03	0.52	0.03	0.36
Cu_{tot}	11.375	11.433	10.623	10.948	9.520	9.265	10.055	9.777

bdl denotes that content of element is below detection limit; Bi is not detected. ***fe*** = Fe/(Fe + Zn); ***sb*** = Sb/(Sb + As).

2.1. Porphyry stage

The porphyry stage Tt_s occurred as large up to 500 μm in size irregular shaped aggregates are rare. Tt_s overgrows and replaces chalcopyrite and forms stringers up to 50 μm in thickness and a few mm in length, which cut chalcopyrite. Electron microscopy identified several generations of the porphyry stage Tt_s (Fig. 6a, b). The first generation Tt_s occurs as large unzoned crystals up to 200 μm in size; it replaces bornite (Fig. 6b) or chalcopyrite I associated with molybdenite (Fig. 6a). It corresponds in chemical composition to Sb- and Zn-poor tennantite with the *sb* value below 0.01 and the *fe* value ranging from 0.60 to 0.80. The Cu_{excess} value widely varies from 0.12 to 1.16 apfu; in the case of bornite replacing it ranges from 0.82 to 1.16. Occasionally this Tt_s generation is enriched in Bi (0.21–0.51 apfu) (Table 2). The second generation Tt_s occurs as tracery aggregates with chalcopyrite II up to a few hundred μm in size (Fig. 6a). It replaces Tt_s I and is replaced by chalcopyrite III. Unfortunately due to close intergrowth with chalcopyrite we were failed in correct measurements of its composition. The third generation Tt_s rims both Tt_s I and II and fill fractures in chalcopyrite III. The rims are oscillatory zoned with the width of separate zones below 20 μm (Fig. 6c). The zoning is caused by variable Sb and As contents with nearly constant Fe and Zn concentrations (Fig. 6d). This generation corresponds to Fe-rich tennantite in chemical composition with the *sb* and *fe* values ranging from 0.19 to 0.37 and from 0.56 to 0.66, respectively. The Cu_{excess} content is low reaching only 0.08 apfu. The Sb and As concentrations range from 1.19 to 1.39 apfu and from 2.48 to 2.66 apfu, respectively in light zones and from 0.72 to 0.88 apfu and from 2.96 to 3.10 apfu, respectively, in dark zones of the rims. The Fe and Zn concentrations are within the narrow ranges from 1.05 to 1.15 apfu and from 0.60 to 0.80 apfu, respectively (Table A1). The fourth generation Tt_s epitaxially overgrowing Tt_s III is characterized by the less pronounced oscillatory zoning as compared with the latter; however, it is also resulted from variable Sb and As contents and negligible variations in the Zn and Fe concentrations (Fig. 6c,d). Compositionally, Tt_s IV corresponds to tetrahedrite with the *sb* and *fe* values varying from 0.51 to 0.70 and from 0.39 to 0.66, respectively. The Cu_{excess} content is similar to that in Tt_s III not exceeding 0.08 apfu. The Sb and As concentrations range from 2.57 to 2.72 apfu and from 1.18 to 1.33 apfu, respectively in the light zones and from 1.97 to 2.06 apfu and from 0.78 to 0.99 apfu, respectively, in the darker zones.

The Tt_s with the *sb* and *fe* values ranging from 0.68 to 0.80 and from 0.30 to 0.35, respectively replacing Tt_s I developed after bornite (Fig. 6b) is close in composition to Tt_s IV. However in this case the Cu_{excess} value is 0.20–0.25 apfu.

Thus, the porphyry stage Tt_s is tennantite and tetrahedrite of four generations with the *sb* and *fe* values ranging from 0 to 0.79 and from 0.28 to 0.80, respectively with gradual increased *sb* value and decreased *fe* value. The Ag concentration in all generations does not exceed a few hundredths apfu. The Cu_{excess} content in the most compositions is as low as a few tenths apfu, but it reaches 1.16 apfu when Tt_s I replaces bornite (Table 2).

2.2. Transitional stage

The transitional stage Tt_s occurred as grains and aggregates varying from 10 to 500 μm in size is typical but minor constituent of the transitional mineral assemblage. It forms inclusions up to 10 μm in pyrite, fills interstices between sphalerite and galena and fractures in these minerals and in chalcopyrite (Figs. 5c, 7a, b), and overgrows earlier porphyry-stage bornite (Fig. 7c). The Tt_s aggregates exhibit at least three generations (Fig. 7d).

The first generation Tt_s with *sb* 0.56–0.80 and *fe* 0.03–0.05 is replaced by weakly zoned Sb-richer Tt_s II with *sb* 0.79–0.82 and *fe* 0.03–0.04 which also fills fractures in Tt_s I. Then the both generations were fractured and the third generation Tt_s depleted in Sb (*sb* 0.03–0.19) and enriched in Fe (*fe* 0.11–0.13) filled fractures. The Ag content in these Tt_s generations The Ag content in Tts I and II is below detection limit by electron microprobe, whereas in Tt_s III it reaches 0.2 wt%.

Tt_s close in composition to the described Tt_s III overgrows bornite of the porphyry stage as unzoned rims associated with hessite and native gold (Fig. 7e). It corresponds to Zn-rich tennantite with the *sb* and *fe* values varying from 0.09 to 0.24 and from 0.07 to 0.09, respectively. In contrast to the porphyry-stage Tt_s replacing bornite, the described Tt_s depleted in Cu_{excess} ranging from 0.05 to

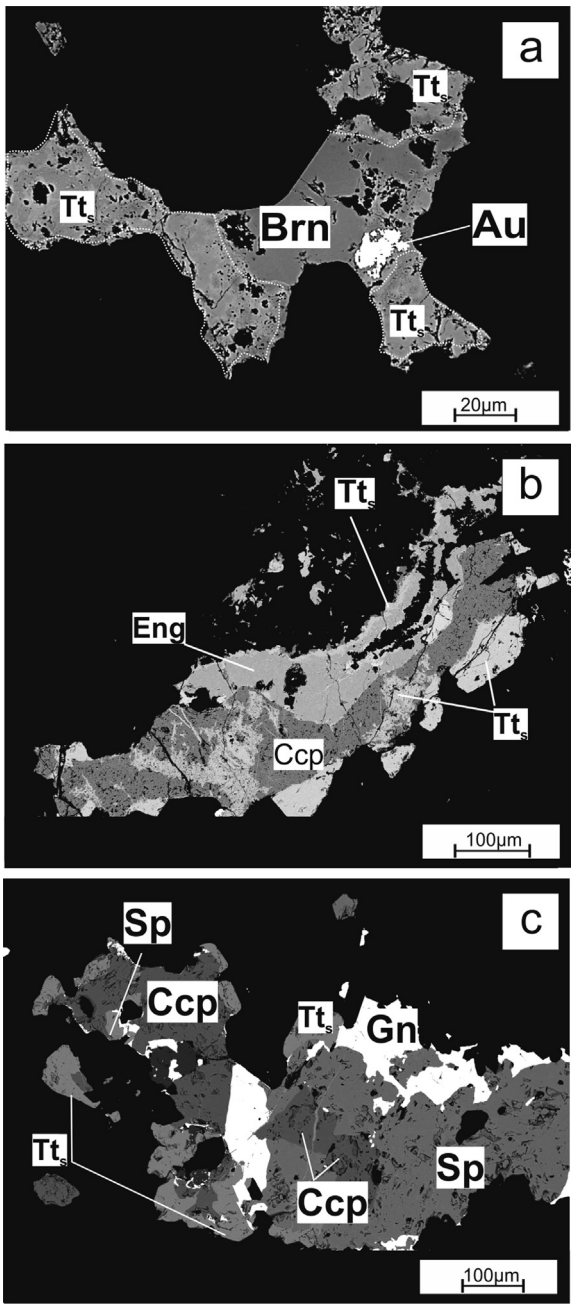

Fig. 9. Back-scattered electron images of (a,b) HS Tts from the Peschanka deposit and (c) IS stage Tt_s. from the Vesenny deposit. (a) Tt_s associated with high-fineness gold replaces bornite, (b) Tt_s tetrahedrite solid solution replacing chalcopyrite and enargite, (c) galena and sphalerite deposited after chalcopyrite; sphalerite is rimmed by Tt_s. See Figs. 2 and 3 for abbreviations.

0.28 apfu Tt_s replacing this Zn-rich tennantite occurred as oscillatory zoned grains (Figs. 7e, 8a) could be referred to generation IV. The width of zones ranges from 3 to 40 μm. Similar to the porphyry stage Tt_s III, zoning is caused by variable Sb and As concentrations with nearly constant Fe and Zn contents (Fig. 8b). Compositionally, this Tt_s is intermediate between tennantite and tetrahedrite with the *sb* and *fe* values varying from 0.03 to 0.69 and from 0.09 to 0.11. The Sb and As concentrations range from 2.62 to 2.95 apfu and from 1.02 to 1.51 apfu, respectively in the light zones and from 0.12 to 0.28 apfu and from 3.24 to 3.81 apfu, respectively, in the darker zones (Table A1). The Ag concentration in Tt_s IV reaches 0.3 wt%. The Cu_{excess} value is close to that in Tt_s III varying from 0 to 0.25 apfu.

Tt_s similar in composition to that of transitional Tt_s III and that overgrowing bornite overgrows galena (Fig. 7f). It is Zn-rich Cu_{excess}-free tennantite (*sb* 0, *fe* 0.12–0.31). Under of effect of late Ag- and Te-bearing solutions at the contact between galena and this Zn-rich tennantite, altaite, hessite, and goldfieldite (Tt_s V, Table 3) are formed (Fig. 7f). The *sb* and *fe* values and Ag concentration in goldfieldite are 0, 0.13, and 0.42 wt%, respectively.

In addition we have identified rare enriched in Bi (up to 0.75 apfu) and Sb-, Ag-, and Cu_{excess}-free tennantite with the low *fe* value ranging from 0.12 to 0.28 that is associated with hessite and petzite (Fig. 7g). Sporadic Te-bearing tennantite (up to 1.39 apfu Te) with the *sb* and *fe* values varying from 0.04 to 0.08 and from 0.18 to 0.19, respectively is associated with galena and sphalerite.

Summarizing the data of transitional-stage fahlores, we conclude that they exhibit five generations. In contrast to the porphyry-stage Tt_s, they are rich in Zn with the *sb* and *fe* values ranging from 0 to 0.82 and from 0.03 to 0.38, respectively. The first and second generations belong to tetrahedrite; the third generation corresponds to tennantite that is occasionally enriched in Bi; the fourth generation is oscillatory zoned tennantite-tetrahedrite; and the fifth generation is goldfieldite and Te-bearing tennantite. The Ag content in transitional fahlores slightly increases to the late generation. Most compositions are depleted in Cu_{excess} in exceptionally separate grains, where its content in Te-bearing Tt_s and goldfieldite reaches 1.39 and 2.14 apfu, respectively.

2.3. Epithermal stage

The *HS* epithermal stage Tt_s occurred as rare unzoned grains up to 300 μm in size replacing enargite and chalcopyrite is associated with high-fineness native gold (910–953) (Fig. 9a,b). Compositionally, it corresponds to Fe-rich tennantite with the very low *sb* value

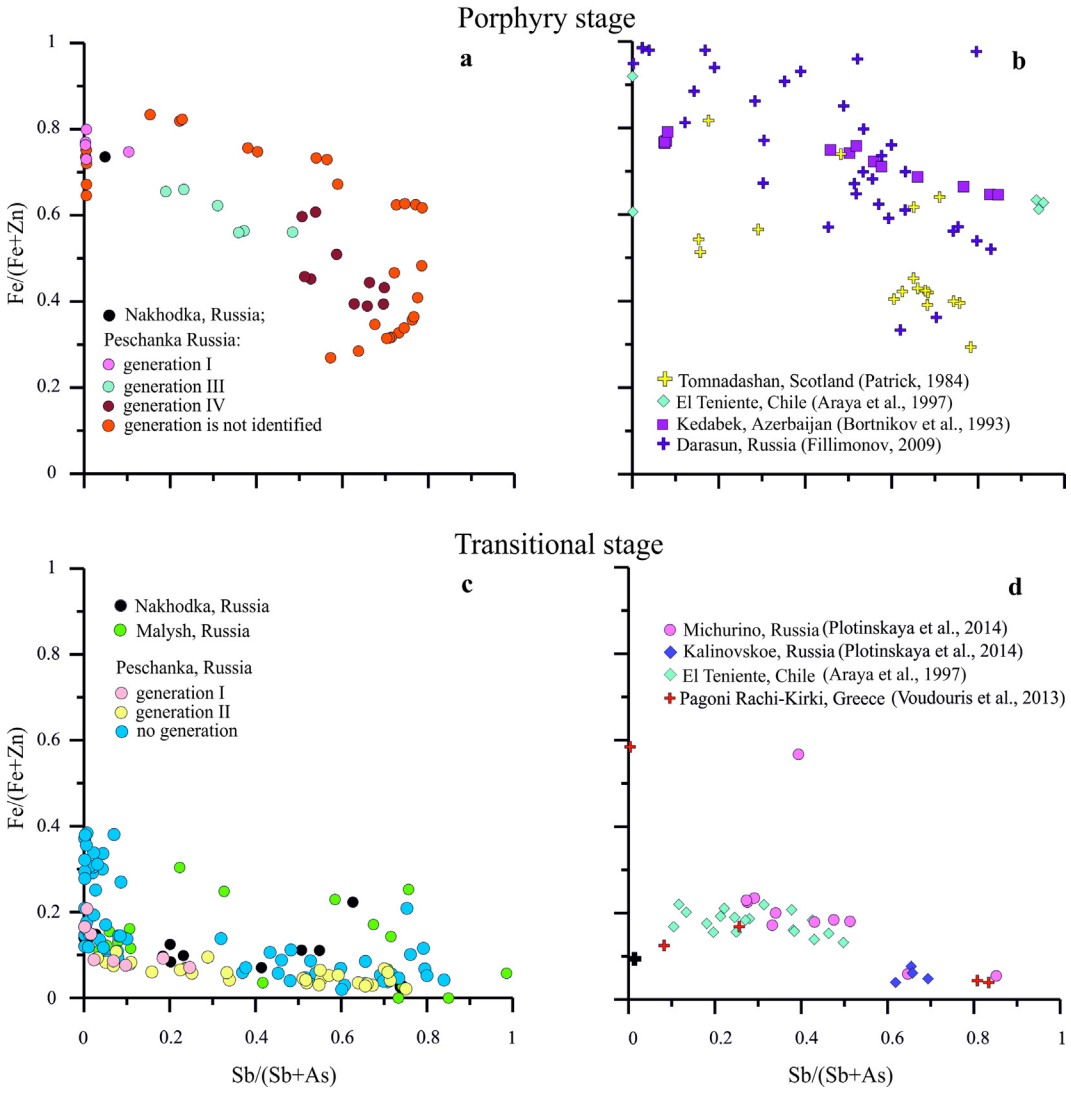

Fig. 10. The Fe/(Fe + Zn) versus Sb/(Sb + As) plots for Tt_s: of porphyry and transitional stage. The second generation of porphyry-stage Tt_s is not shown due to fail in correct measurement of its composition.

below 0.05 and the high *fe* value of 0.65 to 1.00. The Cu_{excess} content is similar to that in the porphyry stage Tt_s reaching 1.43 apfu. The Ag concentration does not exceed 0.03 apfu (Table 3).

The *IS* or *carbonate-base metal Au epithermal* stage Tt_s with the grain size below 50 μm is enclosed in zoned As-bearing pyrite, fills fractures in chalcopyrite, and replaces sphalerite (Fig. 9c). Tt_s is common constituent of the IS ore. Compositionally, it corresponds to Zn-rich tennantite or tetrahedrite with the *sb* and *fe* values varying from 0 to 0.97 and from 0.03 to 0.44, respectively. The Cu_{excess} content does not exceed a few hundredths apfu (Table 3). Silver-bearing (2.6–4.1 wt% Ag) Zn-rich tetrahedrite with the *sb* and *fe* values varying from 0.52 to 0.97 and from 0.08 to 0.27, respectively was found at the Vesenny deposit.

3. Discussion

Similarly to Tt_s grains at the Baimka deposits the oscillatory zoning caused by the variable Sb and As contents was indentified previously in tetrahedrite of the El Teniente porphyry copper deposit in Chile (Araya et al., 1977), Tt_s of the Bugdaya Mo-W-Au porphyry deposit in Russia (Kovalenker et al., 2011), and Tt_s at the lower level of the Baia Sprie epithermal Au deposit in Romania (Buzatu et al., 2015). The compositional heterogeneity was observed in the tetrahedrite-group minerals at the other type hydrothermal deposits. For example, Mozgova and Tsepin (1983a,b) and Spiridonov et al. (2009) reported Tt_s with oscillatory zoning at the Darasun porphyry gold deposit, where the zoning results from the variable Sb, As, Zn, and Fe contents. Zoned Tt_s described from the Berezovsky, Russia and Bestobe, Kazakhstan mesothermal gold deposits (Spiridonov et al., 2009) is characterized by the grains of the tetrahedrite-group minerals by the subtle gradual increasing Ag concentration toward the rims and zonation grains caused by the variable Sb and As concentrations. At the Elshitsa, Bulgaria, and Prasolovskoe and Ozernovskoe, Russia epithermal gold deposits and Madan skarn deposit, Bulgaria, which are not related to known porphyry system, oscillatory zoned Te-bearing Tt_s including goldfieldite is caused by variable contents of the elements at the *X* site (Te, As, Sb, Bi) and/or *B* site (Hg, Fe,

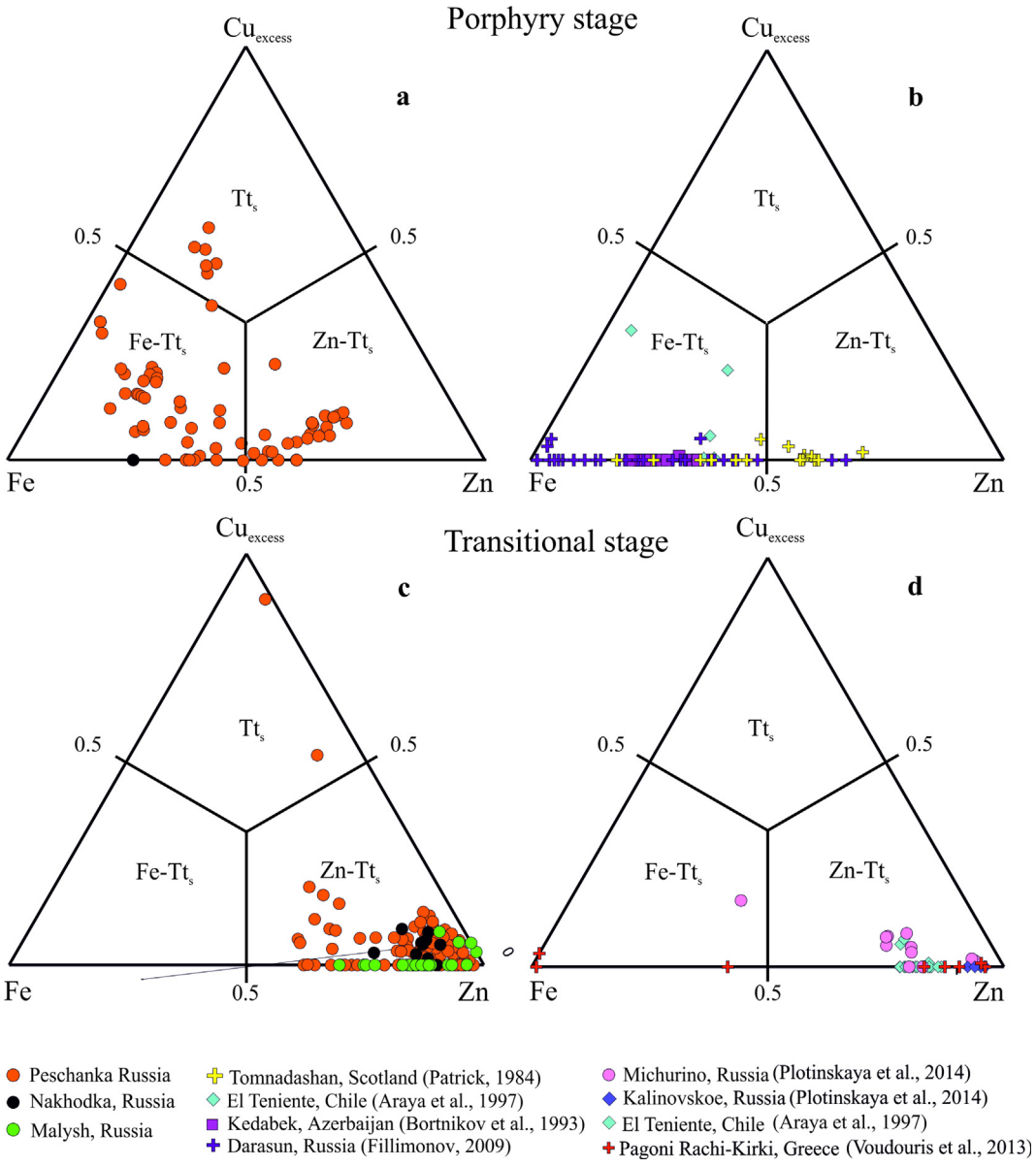

Fig. 11. Ternary diagrams in terms of Fe-Cu_{excess}-Zn for Tt_s of porphyry and transitional stage.

Zn) (Plotinskaya et al., 2005; Spiridonov et al., 2009; Fillimonov, 2009; Vassileva et al., 2014). The comparison of heterogeneous compositions of the tetrahedrite-group minerals from various types of hydrothermal deposits suggests oscillatory zoning caused by exclusive variation in the Sb and As contents is typical of only the porphyry and transitional stage Tt_s at the porphyry copper deposits. The reasons for oscillatory zoning are currently unclear. Shore and Fowler (1996) reported the major reasons as extrinsic (e.g., change in solution composition, pressure or temperature) and intrinsic (e.g., adsorption of growth inhibitors) mechanisms. According to Plotinskaya et al. (2005, 2015) and Buzatu et al. (2015), the oscillatory zoning of the tetrahedrite-group minerals is caused by variable activities of As and Sb in mineralizing fluid due to growth rate kinetics of the fahlore crystals, controlled by the concentrations of these elements in the reaction zone of growing crystals. In addition, Reeder et al. (1990) suggest the oscillatory zoning is only possible crystals formed from unstirred solutions.

3.1. Comparison of the chemical composition of Tt_s studied here and that from other porphyry and epithermal deposits has identified several features

A Fe/(Fe + As) versus Sb/(Sb + As) plot (Fig. 10b) shows that the Tt_s compositions from porphyry copper deposits Kedabek, Azerbaijan (Bortnikov et al., 1993), El Teniente, Chile (Araya et al., 1997), and Tomnadashan, Scotland (Pattrick, 1984), and the Darasun porphyry gold deposit, Russia (Fillimonov, 2009) evolve similarly to the porphyry stage Tt_s at the Peschanka deposit (Fig. 10a). The Tt_s compositions evolve from Fe-rich tennantite to Zn-rich tetrahedrite caused increasing f_{S2} (Krismer et al., 2011) and Sb accumulation in hydrothermal solution. The Tt_s compositions from porphyry deposits on the ternary diagram in terms of Fe-Cu_{excess}-Zn fall predominantly into the Fe-rich Tt_s field (Fig. 11a,b) and to lesser extent, into the Zn-rich Tt_s field and are poor in Cu_{excess}. Thus, the compositional

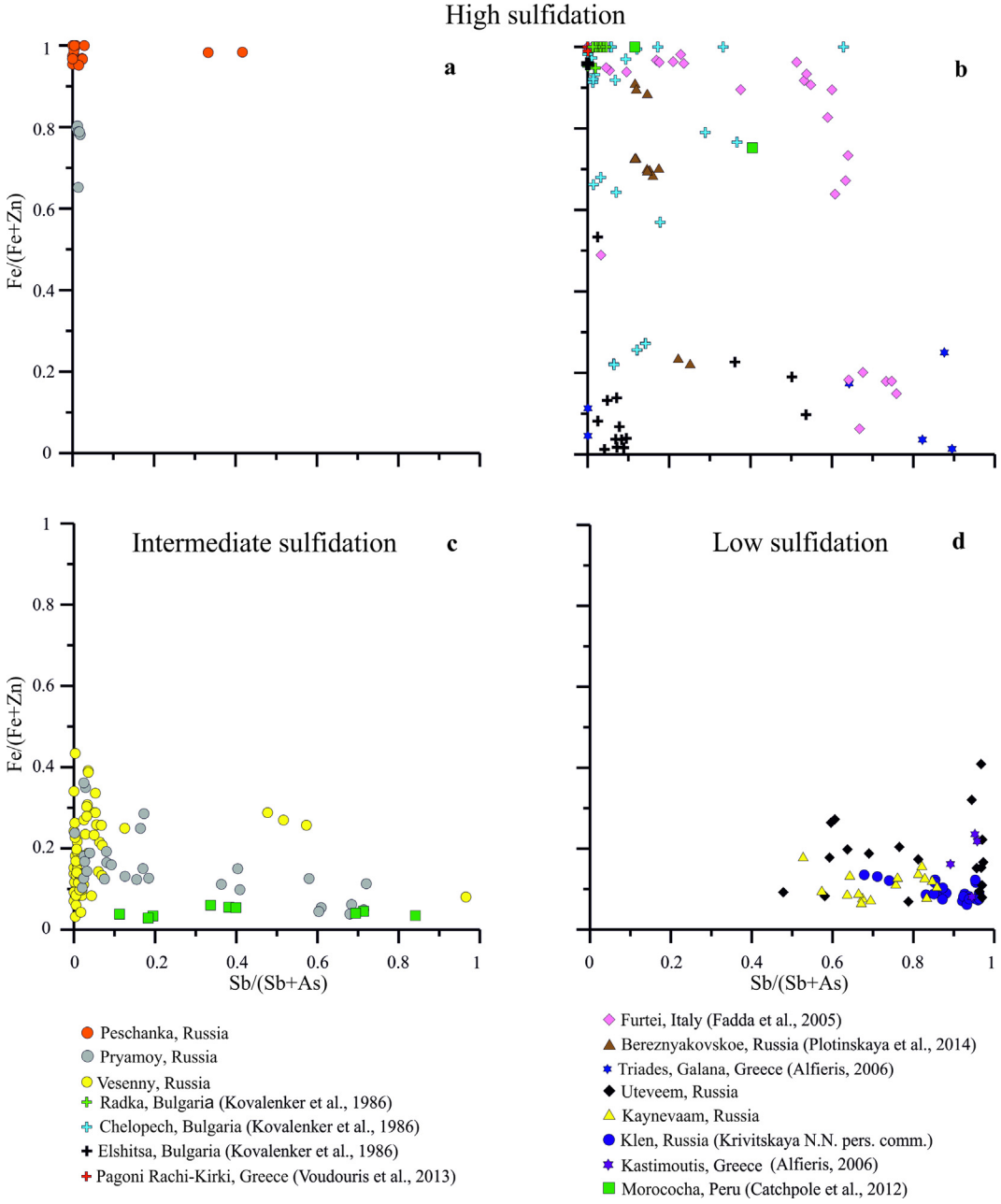

Fig. 12. The Fe/(Fe + Zn) versus Sb/(Sb + As) plots for the epithermal high, intermediate, and low sulfidation, Tt_s.

trend from Fe-rich tennantite to Zn-rich tetrahedrite is considered to distinguish porphyry-type mineralization from other hydrothermal types.

Tetrahedrite-group minerals associated with base-metal sulfides were reported at the Kalinovskoe (Plotinskya et al., 2014) and El Teniente (Araya et al., 1997) porphyry copper deposits where associated sulfide (galena, sphalerite, chalcopyrite) and gangue (dolomite, calcite, tourmaline) minerals represent transitional stage mineralization. In addition, Plotinskya et al. (2014) reported Tt_s from the Michurino Au-Ag prospect that was previously referred to as subepithermal (transitional) type (Plotinskaya and Grabezhev, 2013). The tetrahedrite-group minerals of the transitional (subepithermal) stage are distinguished from those of the porphyry stage by lower *fe* values reaching only 0.4. The Fe/(Fe + As) versus Sb/(Sb + As) binary plots (Fig. 10c,d) show that the compositions of transitional Tt_s are nearly parallel to the Sb/(Sb + As) axis. On the ternary plot in terms of Fe-Cu_{excess}-Zn, these compositions fall into the Zn-rich Tt_s field and are characterized by the higher Zn concentration as compared with those of the porphyry stage (Fig. 11c,d).

Transitional and IS or carbonate—base-metal Au stage show different evolution. The first evolves from Zn-rich tetrahedrite through Zn-rich tennantite followed by oscillatory zoned tennantite-tetrahedrite to goldfieldite, whereas the second evolves from Zn-rich tennantite to Zn-rich tetrahedrite. The evolution of the transitional-stage Tt_s indicates fluctuations in As and Sb regime in fluid, whereas evolution of the IS-stage Tt_s is caused by the gradual Sb accumulation in fluid during mineralizing process. According to Nikolaev et al. (2016), the IS ore at the Vesenny deposit contains hessite, stützite, and petzite. Taking into account this fact and presence of telluride minerals at the transitional stage, we conclude the increased f_{Te2} to the end of both transitional and IS stages within the Baimka trend. The compositions of the IS stage Tt_s from the Vesenny deposit and Pryamoy prospect deposits within the Nakhodka ore field, and Morococha porphyry deposit in Peru (Catchpole et al., 2012) lie in a similar position on diagrams (Figs. 12c, 13c, 15c). Late Ag-bearing IS tetrahedrite found at the Vesenny and Morococha deposits indicates increasing Ag activity in fluid and could be proposed as criterion to distinguish transitional and IS Tt_s along with the As concentration in pyrite and

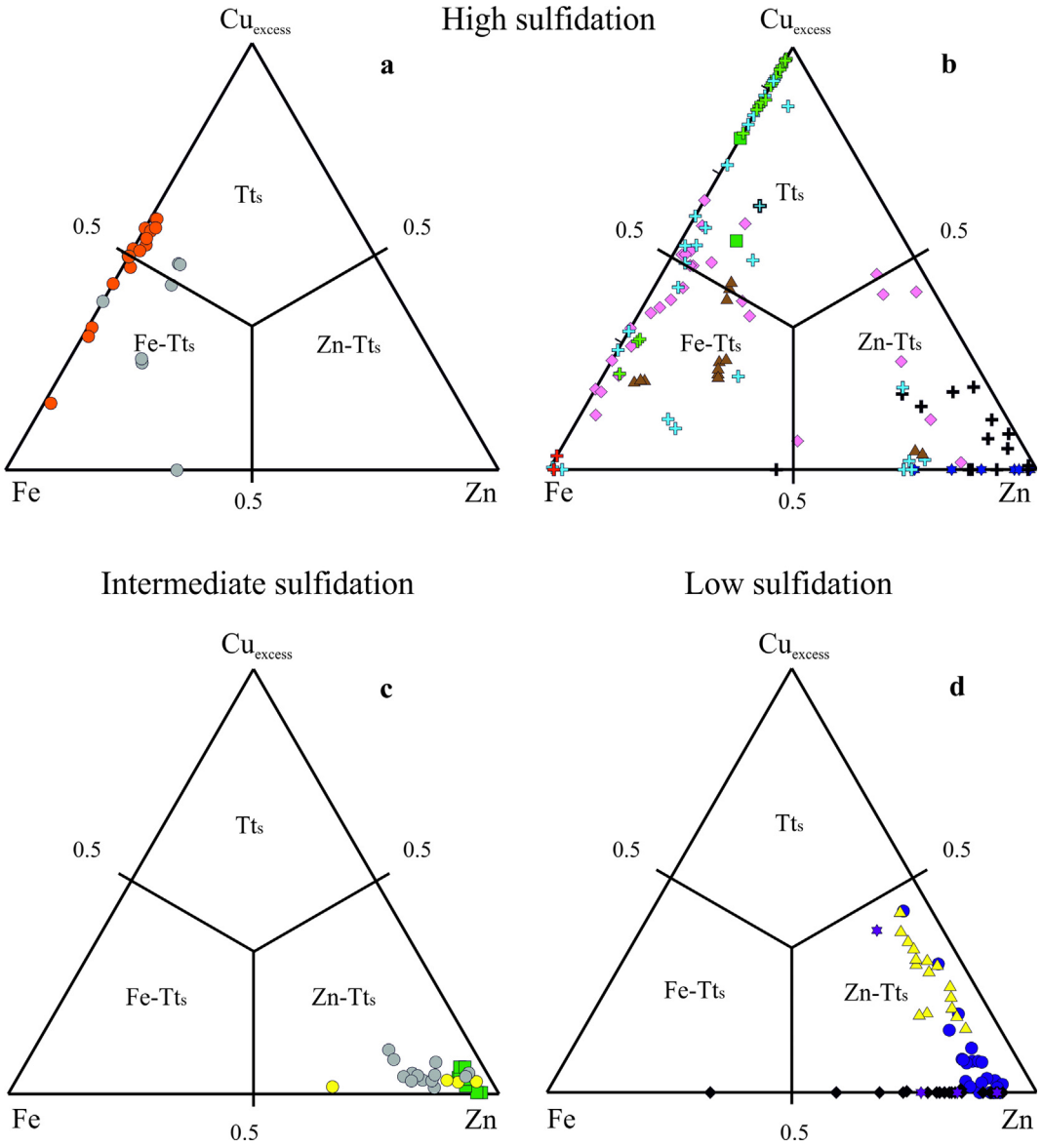

Fig. 13. Ternary diagrams in terms of Fe-Cu_{excess}-Zn for the epithermal high, intermediate, and low sulfidation, Tt_s: See Fig. 10 for legend.

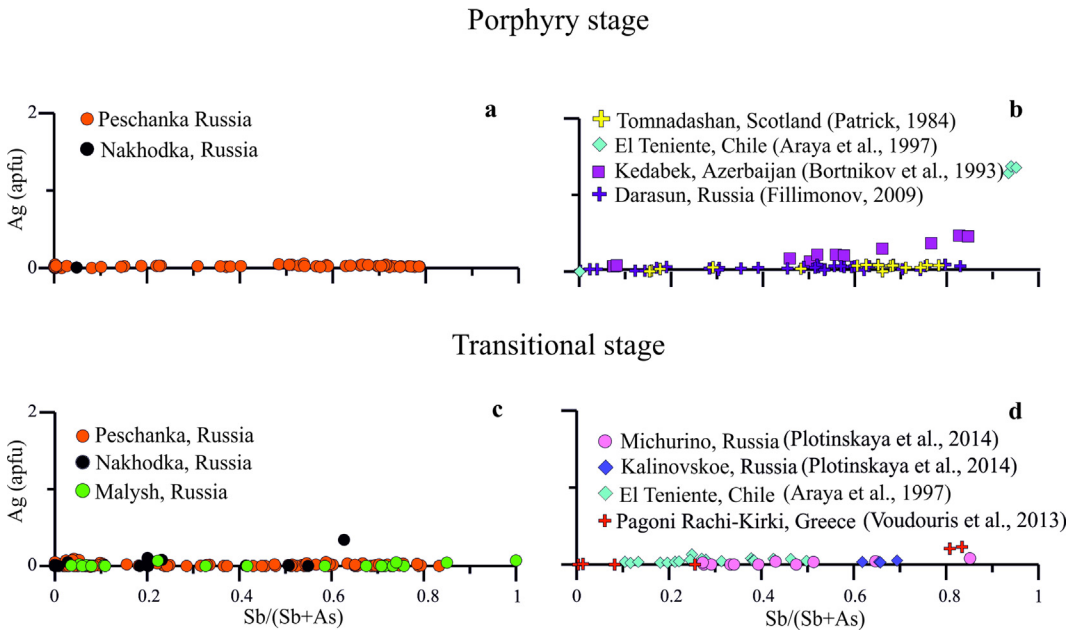

Fig. 14. The Ag versus Sb/(Sb + As) diagrams for porphyry and transitional stage Tt_s.

carbonate composition (Marushchenko et al., 2015). In the transitional Tt_s, Ag content is close or below detection limit by electron microprobe (Fig. 14).

Transitional- and IS-stage minerals at the Peschanka deposit and Nakhodka ore field probably precipitated at similar temperature. Homogenization temperature of inclusions in transitional-stage quartz from the Peschanka deposit and in IS sphalerite from the Vesenny deposit is identical ranging from 160 to 290 °C and from 160 to 280°C, respectively (Nikolaev et al., 2016).

The HS stage Tt_s evolves from Cu_{excess}-bearing Fe-rich tennantite to Cu_{excess}-free Zn-rich tennantite of tetrahedrite at deposits with abundant HS mineralization, such as Furtei in Italy (Fadda et al., 2005), Bereznyazkovskoe in Russia (Plotinskya et al., 2014), Chelopech, Elshica, and Radka in Bulgaria (Kovalenker et al., 1986), and Marococha in Peru (Catchpole et al., 2012). On the Fe/(Fe + As) versus Sb/(Sb + As) plot (Fig. 10b), the compositions of the early HS Tt_s is consistent with the early Tt_s of the porphyry stage, while the late HS Tt_s compositions at this diagram are similar to those of the transitional stage. However, the HS Tt_s compositions on the ternary plot in terms of Fe-Cu_{excess}-Zn (Fig. 11a,b) fall predominantly into the Cu_{excess}- and Fe-rich Tt_s fields, whereas the porphyry stage compositions fall predominantly into the Fe-rich Tt_s field and to less extent, into the Zn-rich Tt_s field; and the transitional stage compositions occupy the Zn-rich Tt_s field (Fig. 9c,d).

The HS stage Tt_s compositions from Peschanka deposit and the Pryamoy deposit within the Nakhodka ore field are characterized by the high *fe* value (0.65–1.0), low *sb* value (up to 0.05), and high Cu_{excess} content (Figs. 10a, 11a). These data are consistent with those for the early HS Tt_s (Fadda et al., 2005, Plotinskya et al., 2014, Kovalenker et al., 1986; Catchpole et al., 2012).

According to Sillitoe and Hedenquist (2003), the LS epithermal mineralization could be a part of the porphyry-epithermal system. For example, it was found at the Kastimoutis prospect in Greece, where Alfieris (2006) reported Tt_s. At Peschanka and within the Nakhodka ore field the LS epithermal mineralization was not found although it was identified within the Baimka trend (Nikolaev et al., 2016). Therefore we compared the composition of the Kastimoutis Tt_s with the Tt_s compositions from the Kaynevaam, Uteveem and Klen LS prospects located within the Chukchi-Okhotsk Volcanic Belt in the Chukchi Peninsula. The Fe/(Fe + As) versus Sb/(Sb + As) plot (Fig. 12d) shows the evolution trend of this Tt_s differed from that of porphyry, transitional, HS and IS compositions. The LS Tt_s compositions evolve from Zn-rich to Fe-rich tetrahedrite probably indicating decreasing f_{S2}. In addition, the LS Tt_s are enriched in Ag reaching 20 wt% to the end of hydrothermal process as compared with the porphyry, transitional, HS, and IS compositions (Figs. 14 and 15). The Ag content is as high as a few hundredths apfu in the porphyry and transitional Tt_s. Ag accumulates in the HS and IS Tt_s toward the late generations, but its concentration is significantly lower than that in the LS tetrahedrite (Fig. 15).

4. Conclusions

The tetrahedrite-group minerals from the porphyry deposits of the Baimka Cu-Mo-Au trend allow the following conclusions. The porphyry and transitional stage Tt_s are characterized by the oscillatory zoning caused only by the variable Sb and As concentrations unlike that of Tt_s from epithermal deposits appear to not be related to porphyry systems and porphyry gold deposits, where the zoning results from the variable contents of elements at the *X* (Te, As, Sb, Bi) and/or *B* site (Hg, Fe, Zn). This criterion could be used to distinguish porphyry copper deposit from other type deposits. The porphyry stage Tt_s, including that of porphyry gold deposits evolves from Fe-rich tennantite to Zn-rich tetrahedrite, whereas the HS epithermal stage Tt_s evolves Fe-rich tennantite to Zn-rich tennantite. The trend from Fe-rich tennantite to Zn-rich tetrahedrite is considered to distinguish porphyry deposits from other type deposits containing tennantite-tetrahedrite solid solution. Early generation of both porphyry and HS Tt_s is enriched in Cu_{excess} caused by replacement of bornite and enargite, respectively. The transitional-stage Tt_s evolves from Zn-rich tetrahedrite through Zn-rich tennantite followed by oscillatory zoned tennantite-tetrahedrite to goldfieldite, whereas the IS-stage fahlores evolve from Zn-rich tennantite to Zn-rich tetrahedrite with increasing Ag concentration. The transitional and IS Tt_s is associated with As-free and As-rich pyrite, respectively. The chemical compositions of fahlores and/or associated minerals indicate increased f_{Te2} to the end of the transitional and IS stages within the Baimka trend. The LS epithermal Tt_s evolves from Zn-rich tetrahedrite to Fe- and

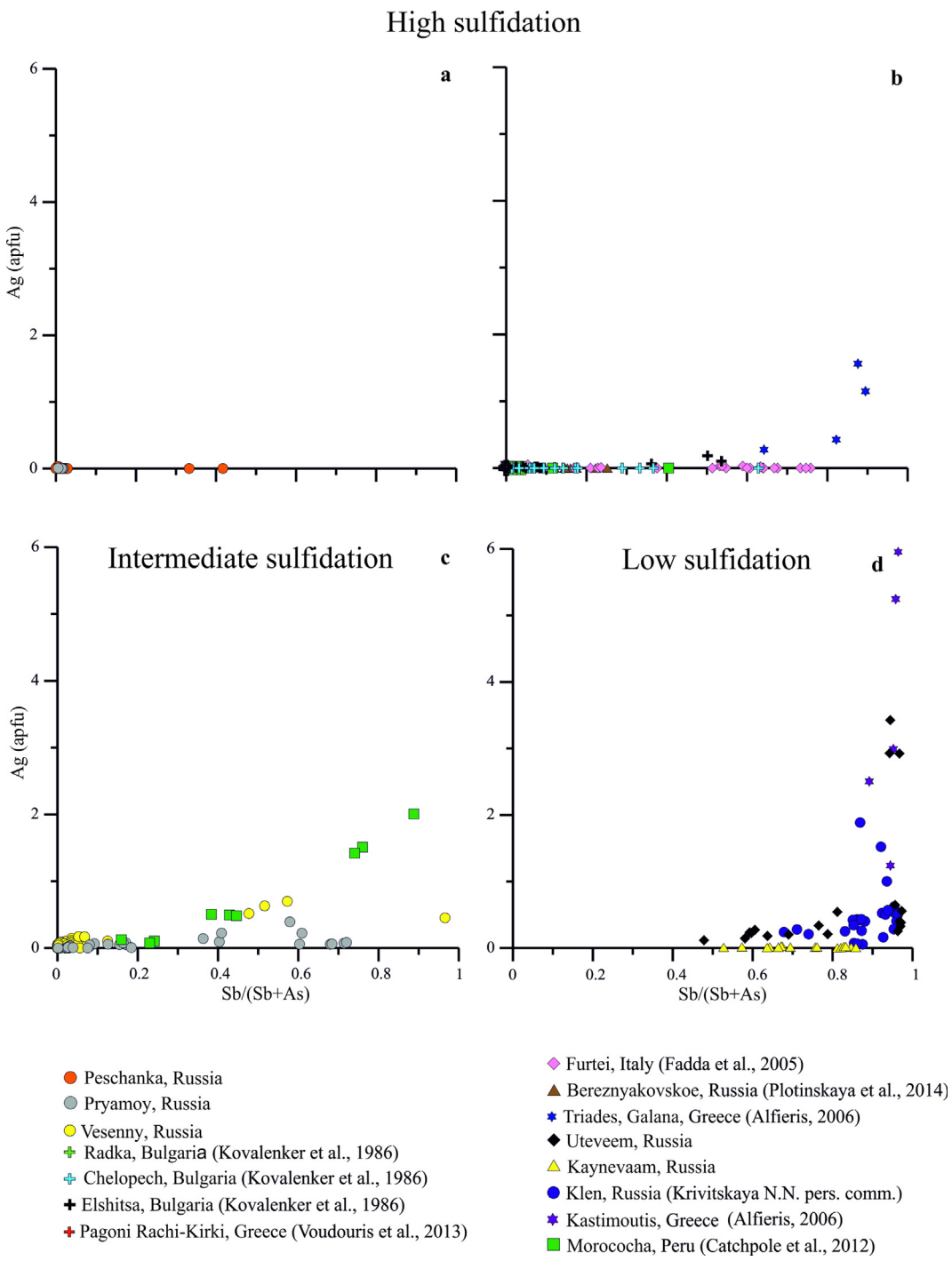

Fig. 15. The Ag versus Sb/(Sb + As) diagrams for the epithermal high, intermediate, and low sulfidation, Tt_s.

Ag-rich tetrahedrite. The character of the compositional evolution of Tt_s is considered as a criterion to separate porphyry, transitional, and epithermal HS, IS, and LS stages. The evolution from tennantite to tetrahedrite at the porphyry and IS stages is caused by the Sb accumulation in fluid, whereas concentrations of Fe and Zn are the function of f_{S2} in mineralizing fluid: the higher f_{S2} the higher Zn concentration. Enrichment of the late IS (or carbonate-base metal Au) and especially LS Tt_s in Ag indicates elevated Ag activity during their formation in contrast to the deposition of the porphyry, transitional, and HS Tt_s.

Acknowledgments

We thank Nadezda Krivitskaya for the fahlore chemical composition from the Klen epithermal LS prospect, Russia, and Olga Plotinskaya and Greg Corbett whose constructive comments significantly improved the manuscript. The purchase of a Jeol JXA-8230 electron microprobe was financially supported by the Program for Development of Lomonosov Moscow State University. This study was supported by the Russian Foundation for Basic Research (project no. 14-05-31198a) and the Baimka Mining Company, LLC.

Appendix A

Table A1
Electron microprobe data for tetrahedrite solid solution of porphyry and transition assemblage from Baimka Cu-Mo-Au trend.

Stage	Porphyry							Transitional (subepithermal)				
Generation	III				IV			IV				
Comp. wt%	1	2	3	4	5	6	7	1	2	3	4	5
Cu	41.51	41.75	42.96	39.71	40.24	39.94	40.62	42.43	39.22	39.59	41.44	42.88
Ag	0.10	0.15	0.19	0.17	0.20	0.17	0.28	0.11	0.21	0.08	0.11	0.15
Fe	3.81	3.65	4.19	2.63	2.90	2.61	2.98	0.67	0.26	0.34	0.31	0.45
Zn	3.43	3.35	2.57	4.75	4.11	4.69	4.13	7.52	7.94	8.05	7.89	8.03
As	11.96	12.05	15.38	5.58	8.80	6.91	8.95	18.90	7.02	9.57	12.91	16.00
Sb	11.45	10.92	5.78	20.80	15.90	18.95	15.25	0.93	19.78	15.94	10.60	4.79
Te	bdl	bdl	bdl	bdl	bdl	bdl	bdl	0.07	0.22	bdl	0.36	bdl
S	27.51	27.26	27.99	26.51	26.83	26.70	26.81	27.68	25.32	25.84	26.46	27.23
Total	99.77	99.12	99.05	100.15	98.97	99.97	99.03	98.31	99.97	99.40	100.08	99.52
Formula calculated on the basis of 29 atoms												
Cu (A)	9.985	9.979	9.973	9.976	9.970	9.975	9.959	9.984	9.969	9.989	9.984	9.979
Ag	0.015	0.021	0.027	0.024	0.030	0.025	0.041	0.016	0.031	0.011	0.016	0.021
Cu (B)	0.055	0.178	0.250	0	0.039	0	0.119	0.105	0.016	0	0.148	0.271
Fe	1.047	1.010	1.134	0.752	0.821	0.740	0.841	0.181	0.076	0.097	0.086	0.123
Zn	0.807	0.792	0.594	1.158	0.994	1.137	0.996	1.738	1.965	1.965	1.876	1.865
As	2.454	2.487	3.104	1.189	1.856	1.462	1.883	3.811	1.515	2.037	2.676	3.243
Sb	1.446	1.387	0.717	2.724	2.064	2.468	1.975	0.115	2.628	2.089	1.352	0.598
Te	0	0	0	0	0	0	0	0.008	0.028	0	0.044	0
Bi	0	0	0	0	0	0	0	0	0	0	0	0
S	13.192	13.145	13.201	13.189	13.227	13.202	13.185	13.042	12.772	12.858	12.819	12.900
fe	0.57	0.56	0.66	0.39	0.45	0.39	0.46	0.09	0.04	0.05	0.04	0.06
sb	0.37	0.36	0.19	0.70	0.53	0.63	0.51	0.03	0.63	0.51	0.34	0.16
Cu_{tot}	10.040	10.157	10.223	9.976	10.009	9.975	10.078	10.089	9.985	9.989	10.132	10.250

bdl denotes that content of element is below detection limit; Bi is not detected. ***fe*** = Fe/(Fe + Zn); ***sb*** = Sb/(Sb + As).

Stage	Transitional (subepithermal)				
Generation	IV				
Comp. wt%	6	7	8	9	10
Cu	40.86	42.10	39.19	41.81	43.25
Ag	bdl	0.19	0.12	0.05	0.05
Fe	0.30	0.58	0.16	0.51	0.83
Zn	7.82	7.77	7.82	7.74	7.88
As	9.62	17.69	4.62	14.68	18.05
Sb	16.45	3.34	21.94	7.33	2.31
Te	bdl	bdl	bdl	bdl	bdl
S	26.18	27.56	25.23	27.01	27.53
Total	101.24	99.27	99.08	99.13	99.91
Formula calculated on the basis of 29 atoms					
Cu (A)	10	9.973	9.982	9.993	9.993
Ag	0	0.027	0.018	0.007	0.007
Cu (B)	0.091	0.050	0.128	0.131	0.209
Fe	0.086	0.157	0.047	0.139	0.222
Zn	1.876	1.799	1.960	1.823	1.807
As	2.015	3.572	1.012	3.015	3.611
Sb	2.120	0.415	2.954	0.926	0.285
Te	0	0	0	0	0
Bi	0	0	0	0	0
S	12.811	13.004	12.900	12.964	12.867
fe	0.04	0.08	0.02	0.07	0.10
sb	0.51	0.10	0.75	0.24	0.07
Cu_{tot}	10.091	10.023	10.110	10.124	10.202

References

Alfieris, D., 2006. Geological, Geochemical and Mineralogical Studies of Shallow Submarine Epithermal Mineralization in an Emergent Volcanic Edifice, at Milos Island (Western side), Greece Ph.D. Dissertation. University of Hamburg, Hamburg, Germany, pp. 1–211.

Araya, R.A., Bowles, J.F., Simpson, P.R., 1977. Relationships between composition and reflectance in the tennantite-tetrahedrite series of El Teniente ore deposit, Chile. Neues Jahrb. Mineral. Monat. 10, 467–482.

Baksheev, I.A., Nikolaev, Yu.N., Prokof'ev, V.Yu., Marushchenko, L.I., Nagornaya, E.V., Chitalin, A.F., Sidorina, Yu.N., Kalko, I.A., 2014. Porphyry-epithermal copper-molybdenum-gold system of the Baimka trend, Western Chukchi Peninsula. Metallogeny of Ancient and Recent Oceans. In: Proc. 20th Sci. School. Institute of Mineralogy Russian Academy of Sciences, Miass, pp. 108–112 (in Russian).

Bortnikov, N.S., Genkin, A.D., Troneva, N.V., 1993. Tennantite decomposition: evidence from the Kedabek copper deposit. Azerbaijan. Mineral. Petrol. 47, 171–181.

Buzatu, A., Damian, G., Dill, H.G., Buzgar, N., Apopei, A.I., 2015. Mineralogy and geochemistry of sulfosalts from Baia Sprie ore deposit (Romania) – New bismuth minerals occurrence. Ore Geol. Rev. 65, 132–147.

Catchpole, H., Kouzmanov, K., Fontbote, L., 2012. Copper-excess stannoidite and tennantite-tetrahedrite as proxies for hydrothermal fluid evolution in a zoned cordilleran base metal district, Morococha, Central Peru. Can. Mineral. 50, 719–743.

Chitalin, A.F., Usenko, V.V., Fomichev, E.V., 2013. The Baimka ore zone – a cluster of large base and precious metal deposits in the western Chukotka AD. Mineral Res. Ross. Econ. Uprav. 6, 68–73 (in Russian).

Corbett, G.J., Leach, T.M., 1998. Southwest Pacific Rim Gold-Copper Systems: Structure, Alteration, and Mineralization. Econ. Geol. Spec Pub, p. 6.

Fadda, S., Fiori, M., Grillo, S.M., 2005. Chemical variations in tetrahedrite - tennantite minerals from the Furtei epithermal Au deposit, Sardinia, Italy: Mineral zoning and ore fluids evolution. Geokhim. Mineral. Petrol. 43, 80–84.

Fillimonov, S.V., 2009. Fahlore group minerals as an indicator of ore genesis: a case study of hydrothermal gold deposits Ph.D. Dissertation. Lomonosov Moscow State University, Moscow.

Kotova, M.S., Nagornaya, E.V., Anosova, M.O., Kostitsyn, Yu.A., Baksheev, I.A., Nikolaev, Yu.N., Kalko, I.A., 2012. Dating of wall-rock alteration process and ore-bearing granitoids of the Nakhodka ore field, Western Chukchi Peninsula. In: Geochronological isotopic systems, methods of their study, and chronology of geological processes V Russian Isotope Conference in Geochronology, Moscow, pp. 181–184. Abstracts (in Russian).

Kovalenker, V.A., Tsonev, D., Breskovska, V.V., Malov, V.C., Troneva, N.V., 1986. New data on the mineralogy of copper-sulphide deposits Mittelgebirge Central Bulgaria. In: Korzhinsky, D.S. (Ed.), Metasomatism, Mineralogy and Problems of Genesis of Gold and Silver Deposits in the Volcanic Sequences. Nauka, Moscow, pp. 91–110 (in Russian).

Kovalenker, V.A., Kiseleva, G.D., Krylov, T.L., Andreeva, O.V., 2011. Mineralogy and ore formation conditions of the Bugdaya Au-Bearing W-Mo porphyry deposit, Eastern Transbaikal Region. Russia. Geol. Ore Deposits. 53, 93–125.

Krismer, M., Vavtar, F., Tropper, P., Kaindl, R., Sartory, B., 2011. The chemical composition of tetrahedrite-tennantite ores from the prehistoric and historic Schwaz and Brixlegg mining areas (North Tyrol, Austria). Eur. J. Mineral. 23, 925–936.

Marushchenko, L.I., Baksheev, I.A., Nagornaya, E.V., Chitalin, A.F., Nikolaev, Yu.N., Kalko, I.A., Prokofiev, V.Yu., 2015. Quartz–sericite and argillic alterations at the Peschanka Cu–Mo–Au deposit, Chukchi Peninsula. Russia. Geol. Ore Deposits. 57, 213–225.

Mozgova, N.N., Tsepin, A.I., 1983a. Fahlores (Singularities of Chemical Composition and Properties of Minerals). Nauka, Moscow (in Russian).

Nikolaev, Yu N., Baksheev, I.A., Prokofiev, Yu N., Nagornaya, E.V., Marushchenko, L.I., Sidorina, Yu N., Chitalin, A.F., Kal'ko, I.A., 2016. Gold–Silver mineralization in porphyry–epithermal systems of the Baimka trend, western Chukchi Peninsula, Russia. Geol. Ore Deposits 58 (4), 319–345.

Moëlo, Y., Makovicky, E., Mozgova, N.N., Jambor, J., Cook, N., Pring, A., Paar, W., Nickel, E.H., Graeser, S., Karup-Møller, S., Balic-Žunic, T., Mumme, W.G., Vurro, F., Topa, D., Bindi, L., Bente, K., Shimizu, M., 2008. Sulfosalt systematics: a review. Report of the sulfosalt sub-committee of the IMA Commission on Ore Mineralogy. Eur. J. Mineral. 20, 7–46.

Moll-Stalcup, E.J., Lane, L.S., Cecile, M.P., Gorodinsky, M.E., 1995. Geochemistry and U-Pb geochronology of arc-related magmatic rocks, Northeastern Russia. In: Abstr. Geol. Soc. Am. 91st Ann. Cordilleran Section, 27, p. 65.

Mozgova, N.N., Tsepin, A.I., 1983b. Fahlore (Chemical Composition and Properties). Nauka, Moscow (in Russian).

Nagornaya, E.V., Baksheev, I.A., Bryzgalov, I.A., Yapaskurt, V.O., 2012. Minerals of the Au–Ag–Pb–Te–Se–S system of porphyry–copper–molybdenum deposits from the Nakhodka ore field, Chukchi Peninsula, Russia. Moscow Univ. Geol. Bull. 67 (4), 233–239.

Nagornaya, E.V., 2013. Mineralogy and zoning of the Nakhodka Cu-Mo-porphyry field, Chukchi Peninsula Ph.D. Dissertation. Lomonosov Moscow State University, Moscow, pp. 1–171 (in Russian).

Nikolaev, Yu.N., Baksheev, I.A., Prokofiev, V.Yu., Nagornaya, E.V., Marushchenko, L.I., Sidorina, Yu.N., Chitalin, A.F., Kal'ko, I.A., 2016. Gold–silver mineralization in porphyry–epithermal systems of the Baimka trend, Western Chukchi Peninsula, Russia. Geol. Ore Deposits 58 (4), 319–345.

Pattrick, R.D., 1984. Sulphide mineralogy of the Tomnadashan copper deposit and the Corrie Buie lead veins, south Loch Tayside, Scotland. Miner. Mag. 48, 85–91.

Plotinskaya, O.Y., Rusinov, V.L., Kovalenker, V.A., Seltmann, R., 2005. Oscillatory zoning in goldfieldites as a possible indicator of its formation conditions. Au-Ag-Te-Se deposits: IGCP Project 486, Kiten, Bulgaria. Geochem. Mineral. Petrol. 43, 142–147.

Plotinskaya O.Y., Grabezhev, 2013. Porphyry deposits of the Urals. In: 12th SGA Biennial Meeting 2013. Proceedings, 4, 1516–1518.

Plotinskya, O.Y., Grabezhev, A.I., Groznova, E.O., Seltmann, R., Lehmann, B., 2014. The Late Paleozoic porphyry–epithermal spectrum of the Birgilda-Tomino ore cluster in the South Urals, Russia. J. Asian Earth Sci. 79B, 910–931.

Plotinskaya, O.Yu., Grabezhev, A.I., Seltmann, R., 2015. Fahlores compositional zoning in a porphyry–epithermal system: Biksizak occurrence, South Urals, Russia as an example. Geol. Ore Deposits. 57, 42–63.

Reeder, R.J., Fagioli, R.O., Meyers, W.J., 1990. Oscillatory zoning of Mn in solution-grown calcite crystals. Earth-Sci. Rev. 29, 39–46.

Repstock, A., Voudouris, P., Zeug, M., Melfos, V., Zhai, M., Li, H., Kartal, T., Matuszczak, J., 2016. Chemical composition and varieties of fahlore-group minerals from Oligocene mineralization in the Rhodope area, Southern Bulgaria and Northern Greece. Mineral. Petrol. 110, 103–123.

Sack, R.O., Lynch, J.V.G., Foit, F., 2003. Fahlore as a petrogenetic indicator: Keno Hill Ag–Pb–Zn district. Yukon. Canada. Mineral. Mag. 67, 1023–1038.

Shore, M., Fowler, A.D., 1996. Oscillatory zoning in minerals: a common phenomenon. Can. Mineral. 34, 1111–1125.

Sillitoe, R.H., Hedenquist, J.W., 2003. Linkages between volcanotectonic settings, ore-fluid compositions, and epithermal precious metal deposits. Soc. Econ. Geol. Spec. Publ. 10, 315–343.

Spiridonov, E.M., Filimonov, S.V., Matveev, A.A., Grigoryan, C.V., Tabatabey, H.S., 2005. Chemical features of fahlores from the Shaumyan, South Armenia and Kharvana, Northwestern Iran gold–base metal massive sulfide deposits. Zap. RMO 134 (3), 85–94 (in Russian).

Spiridonov, E.M., Filimonov, S.V., Bryzgalov, I.A., Guseva, E.V., Korotaeva, N.N., Krivitskaya, N.N., Yapaskurt, V.O., 2009. Zoning of the fahlore group minerals as a criteria for distinction between plutonogenic, volcanogenic-plutonogenic and volcanogenic hydrothermal gold deposits. In: Marin, Yu.B., Morozov, M.V., Petrov, D.A. (Eds.), Ontogeny of minerals applied to scientific and industrial uses (to the 100 year anniversary of Prof. Dmitry Grigoriev). Russian Mineral. Soc., Saint Petersburg, pp. 135–136 (in Russian).

Vassileva, R.D., Atanassova, R., Kouzmanov, K., 2014. Tennantite-tetrahedrite series from the Madan Pb-Zn deposits, Central Rhodopes, Bulgaria. Miner. Petrol. 108, 515–531.

Voudouris, P.C., Melfos, V., Spry, P.G., Kartal, T., Schleicher, H., Moritz, R., Ortelli, M., 2013. The Pagoni Rachi-Kirki Cu-Mo ± Re ± Au deposit, northern Greece: mineralogical and fluid inclusion constraints on the evolution of a telescoped porphyry-epithermal system. Can. Mineral. 51, 253–284.